NC WATER RESOURCES RESEARCH INSTITUTE

Report No. 506

PERFORMANCE EVALUATION OF NOVEL RESINS IN FLOW-THROUGH COLUMNS FOR PFAS REMOVAL FROM DRINKING WATER AND TREATED WASTEWATER

By
Orlando Coronell[1], Frank A. Leibfarth[2], Irene M. Manning[2], Alexander S. Gorzalski[3], Guan Pin Nick Chew[1]

1. Department of Environmental Sciences and Engineering
   Gillins School of Global Public Health
   The University of North Carolina at Chapel Hill
   Chapel Hill, NC

2. Department of Chemistry
   College of Arts and Sciences
   The University of North Carolina at Chapel Hill
   Chapel Hill, NC

3. One Water Engineering, PLLC
   Raleigh, NC

wrri.ncsu.edu
NC WATER RESOURCES RESEARCH INSTITUTE

UNC-WRRI-506

The research on which this report is based was supported by funds provided by the North Carolina General Assembly and/or the US Geological Survey through the North Carolina Water Resources Research Institute.

WRRI Project No. 22-08-W
November 30, 2023

Performance Evaluation of Novel Resins in Flow-Through Columns for PFAS Removal from Drinking Water and Treated Wastewater

(WRRI project#21-14-W)

Prepared by:

Orlando Coronell[a], Professor, PI
Frank A. Leibfarth[b], Associate Professor, PI
Irene M. Manning[b], Lead Research Chemist
Alexander S. Gorzalski[c], Engineering Consultant
Guan Pin Nick Chew[a], Postdoctoral Researcher

[a] Department of Environmental Sciences and Engineering, Gillings School of Global Public Health, The University of North Carolina at Chapel Hill, Chapel Hill, NC 27599
[b] Department of Chemistry, College of Arts and Sciences, The University of North Carolina at Chapel Hill, Chapel Hill, NC 27599
[c]One Water Engineering, PLLC Raleigh, NC 27615

PI's contact information:
Orlando Coronell, coronell@unc.edu
163B Rosenau Hall, CB#7431
Department of Environmental Sciences and Engineering
University of North Carolina at Chapel Hill
Chapel Hill, NC 27599-7431
Tel: 919-0966-9010
Fax: 919-966-7911

Submitted to:

North Carolina Water Resources Research Institute

November 30, 2023

Project Number: 21-14-W
Project title: "Performance Evaluation of Novel Resins in Flow-Through Columns for PFAS Removal from Drinking Water and Treated Wastewater"
PIs: Orlando Coronell and Frank Leibfarth, University of North Carolina at Chapel Hill

Note: A more detailed version of a portion of this report was previously published as the peer-reviewed manuscript Manning, I.M.; Chew, N.G.P.; Macdonald, H.P.; Miller, K.E.; Strynar, M.J.; Coronell, O.; Leibfarth, F.A, *Angew. Chem. Int. Ed.* 2022**,** *61,* e202208150 (DOI: 10.1002/anie.202208150). The published paper and corresponding Supporting Information can be found in Appendix 3.

Abstract

Per- and polyfluoroalkyl substances (PFAS) are known bioaccumulative and persistent chemicals which pollute natural waters globally. However, there exists a lack of granular sorbents optimized to efficiently remove PFAS at environmentally relevant concentrations. To address this need, we previously developed a platform approach for fabrication of regenerable granular sorbents (i.e., ionic fluorogel (IF) resins) that selectively remove PFAS over background competing contaminants. In this project, we modified 1st generation IFs to realize structurally tunable and chemically stable resins with systematic variations of network architecture and cation density. Chemical stability was demonstrated through accelerated degradation studies. Investigation of the library of chemically stable IFs enabled insights into structure–property relationships important to high affinity PFAS binding. Results show that the chemically stable IF resin outperformed a leading commercially available ion-exchange resin in batch and column tests. Using as a guiding principle in sorbent development the cost and availability at large scale of base materials, we developed a 2nd generation IF resin based on trifunctional crosslinkers with a more translationally relevant profile in terms of chemical inputs and cost. Batch results from challenge tests with various NC waters showed that the 2nd generation IF resin had a PFAS-removal performance level intermediate between those of two leading commercial ion exchange resins. The 2nd generation IF resin had a substantially better performance in drinking water sources than in wastewater matrices. Results also showed that there is the potential to improve PFAS removal performance via optimization of the resin synthesis procedure. Additionally, because of the high modularity and copolymerization amenability of the platform chemistry used for IF synthesis, we hypothesize that future tuning of the fluorinated backbone can be used to optimize PFAS partitioning, and resin swelling and flexibility and enable superior PFAS removal across water matrices.

Acknowledgements

This work was supported by the Strategic Environmental Research and Development Program of the U.S. Department of Defense (ER20-1211, F.A.L.), the NC Collaboratory (F.A.L. and O.C.), the National institute of Environmental Health Sciences (P42ES031007, O.C.), and the NC Water Resources Research Institute (WRRI) and US Geological Survey (USGS) (2021-2501-01 and 2021-3441-02, O.C. and F.A.L.). I.M.M. acknowledges the Dobbins Fellowship. The authors thank Dr. Elango Kumarasamy for valuable discussions. The authors thank The Chemours Company for their donation of standards. We also thank Devin Guillory and Abigail Sveen for their assistance with sorbent testing, Sontia Gaither for assistance with synthesis of novel sorbents, and Jenna Demartino for PFAS analysis of water samples. Additionally, we thank James Mccord for his R code that sorts masses into homologous series. The authors thank the City of Burlington, the City of Greensboro, the Cape Fear Public Utility Authority (CFPUA), and the Orange Water and Sewer Authority (OWASA) for assisting with sample collection and lending their expertise to help make our research approach and findings useful to the broader water sector. We also thank Evoqua, Purolite, and Kuraray for providing commercial sorbents. The authors thank the University of North Carolina's Department of Chemistry Mass Spectrometry Core Laboratory for their assistance with mass spectrometry analysis. The UNC Department of Chemistry's NMR Core Laboratory provided expertise and instrumentation that enabled this study with support from National Science Foundation (CHE-1828183 and CHE-0922858). The authors thank Dr. Mark J. Strynar and Dr. Kelsey E. Miller at the Office of Research and Development, Center for Environmental Measurement and Modeling, U.S. Environmental Protection Agency (EPA) for performance of nontargeted analysis. Any mention of trade names, manufacturers or products does not imply an endorsement by the United States Government or the U.S. Environmental Protection Agency.

1. Introduction

PFAS are a diverse class of chemicals that are extensively used in industrial and consumer products ascribing to their oil- and water-repelling properties (Rahman et al., 2014). PFAS are widespread contaminants of air, soil, and water media and they are persistent in the environment, bio-accumulative, and difficult to remove by existing technologies (Evich et al., 2022). Further, exposure to PFAS poses potential adverse health effects including cancer, thyroid disease, pregnancy-induced hypertension and preeclampsia, among others (Grandjean et al., 2012; Barry et al., 2013; National Institute of Environmental Health Sciences, 2022; United States Environmental Protection Agency, 2022a). Accordingly, the U.S. Environmental Protection Agency (EPA) set interim updated lifetime health advisory levels in drinking water of 0.004 and 0.02 ng/L for perfluorooctanoic acid (PFOA) and perfluorooctanesulfonic acid (PFOS), respectively, and a final health advisory level of 10 ng/L for GenX (United States Environmental Protection Agency, 2022b). EPA subsequently proposed maximum contaminant levels (MCLs) of 4 ng/L for PFOA and PFOS, and a hazard index calculated based on the concentrations of GenX, perfluorohexanesulphonic acid (PFHxS), perfluorononanoic acid (PFNA), and perfluorobutane sulfonate (PFBS) (United States Environmental Protection Agency, 2023). In addition, numerous states have set limits on PFAS in drinking water (Boone et al., 2019).

Occurrence studies have detected legacy and emerging PFAS in multiple locations in NC, including drinking water sources (Sun et al., 2016; Dukes, 2017; Hopkins et al., 2018; North Carolina Division of Water Resources, 2018; Seymour Johnson Air Force Base, 2019; Barnes, 2020b; United States Environmental Protection Agency, 2022c). Among U.S. states, NC is the third highest state for PFAS exposure through drinking water (Scruggs, 2019) with North Carolinians being exposed to PFAS through contaminated drinking water supplied by either municipal water treatment systems (City of Raleigh, 2020; Evans et al., 2020; Ross, 2020) or private wells (Sun et al., 2016; MacDonald Gibson and Pieper, 2017; North Carolina Division of Water Resources, 2018; Barnes, 2020a). For example, PFAS have been shown to be present in the Cape Fear River Watershed (Sun et al., 2016; Hopkins et al., 2018; Barnes, 2020b), private wells (North Carolina Division of Water Resources, 2018), groundwater near Seymour Johnson Air Force Base (Seymour Johnson Air Force Base, 2019), Cane Creek Reservoir, streams near Greensboro Airport, Lake Jordan, and drinking water of Cary and Apex (Dukes, 2017). PFAS exposure through private wells is of particular importance since NC has the second-largest population (3.3 million) and third-highest population percentage (35%) who rely on private wells for drinking water (MacDonald Gibson and Pieper, 2017). PFAS have also been found in effluents from wastewater-treatment plants that receive contaminated waters from industrial facilities, therefore contaminating receiving water streams (Southern Environmental Law Center, 2019;

Barnes, 2020b). This is the case, for example, for the South and East Burlington Wastewater Treatment Plants in NC (Southern Environmental Law Center, 2019).

The occurrence of PFAS across different NC water sources, Iing finished drinking water, the large NC population relying on private wells, and the relatively low-income level of the median North Carolinian household (39th in the U.S. in 2021) (World Population Review, 2022), means that technologies for effective PFAS removal from water need to be amenable to easy implementation not just in municipal facilities but also in the average NC household. However, PFAS are recalcitrant to degradation and, in particular, short-chain PFAS are not effectively removed by conventional nor advanced water treatment processes. Hence, a need exists to develop technologies for effective removal of PFAS from water (Yu et al., 2012; Dudley et al., 2015; Sun et al., 2016; Hopkins et al., 2018).

To address PFAS removal technology needs, we recently reported (Kumarasamy et al., 2020) a platform approach for the development of regenerable granular 5luorogelsorogel (IF) resins that effectively removed, in batch tests, a diverse mixture of 21 legacy and emerging PFAS from real water samples, including short-chain PFAS. The IF resins are crosslinked polymers that combine ionic and fluorous components to achieve specificity for PFAS sorption over background organic contaminants. We demonstrated that perfluoropolyether (PFPE)-based IFs could outperform commercial granular activated carbon (GAC) and an ion exchange resin (IX), even in the presence of 20,000 times excess non-fluorinated organic matter (Kumarasamy et al., 2020). However, the PFPE used in the initial proof-of-concept work had a structure containing ester and carbamate linkages which we hypothesized would degrade over long lifetimes in flow-through columns. Additionally, the use of only one PFPE limited systematic evaluation of the influence of network architecture on PFAS sorption and performance tests were not performed in the typical configuration used at full scale (i.e., packed-bed configuration).

In this work, to achieve hydrolytically stable PFPE-IFs, we end-functionalized the 1st generation PFPEs with polymerizable functionality connected through aryl-ether linkages. Subsequent copolymerization of these PFPEs with an amine-containing monomer resulted in a library of IFs with systematic variations of network architecture and cation density. Investigation of this library enabled insights into structure-property relationships important to high affinity PFAS binding. In accelerated degradation studies, the hydrolytically stable PFPE-IF maintained a low swelling ratio and consistent mass, whereas its predecessor degraded significantly, as measured via mass loss and nontargeted analysis using high-resolution mass spectrometry. Finally, in a translationally relevant proof-of-concept experiment, mini-Rapid Small-Scale Column Tests (RSSCTs) of one IF significantly outperformed a state-of-the-art ion-exchange resin by

demonstrating effective PFAS removal from natural NC water over one year of simulated use. We also proposed as an alternative to PFPEs fluoroolefin-vinyl ethers (FVEs) which are partially fluorinated polymers that are components of Lumiflon™ brand paints, cost $20-40 per kilogram (as opposed to ~$500 per kilogram for PFPEs), are chemically stable for decades in outdoor paint application, and do not require PFAS surfactants for their production. Preliminary tests in our laboratories have shown that 2nd generation fluorogels based on FVE polymer networks have the same advantages as PFPE-IFs in terms of PFAS removal selectivity, which enables their use as a materials platform.

Therefore, the overall goal of this project was to develop physically and chemically stable IF resins for PFAS removal from water with translational relevance for use at full scale. We explored further development of PFPE-IFs (1st generation resins) as well as FVE-IFs (2nd generation resins). Specific objectives were to:

(1) develop a systematic library of chemically stable IF resins through end-group modifications
(2) evaluate the efficacy of chemically stable IF resins at removing long-chain and short-chain PFAS from water
(3) evaluate the regenerability of chemically stable IF resins
(4) evaluate the translational relevance of chemically stable FVE-IF resins by assessing their performance in flow-through, packed-bed configuration

2. Materials and Methods

2.1 Materials

All materials were purchased from commercial source and used as received without further purification unless otherwise mentioned. Perfluoropolyether Fluorolink® E10H (Mwt: 1.8-2.0 kg·mol^{-1}) was purchased from Solvay Solexis. Perfluorostyrene was purchased from Oakwood Chemical. 1H,1H,11H,11H-Perfluoro-3,6,9-trioxaundecane-1,11-diol was purchased from Exfluor. 2-(dimethylamino)ethanol, 2-(dimethylamino)ethyl methacrylate, azobisisobutyronitrile (AIBN), humic acid and perfluorooctanoic acid (PFOA) were purchased from Sigma-Aldrich. Trifluoroethanol was purchased from Synquest labs. Perfluorohexanoic acid (PFHxA) and GenX were purchased from TCI and Matrix respectively. Me6TREN was purchased from TCI, and fluoroolefin-vinyl ether copolymers were provided by AGC Chemical company.

Deionized water used in this study is a type 1, 18.2 megohm-cm water obtained from Labconco – waterpro PS series. This water was amended with sodium chloride and humic acid as described for specific experiments. Natural water samples were also collected from diverse water sources for evaluation of PFAS removal by commercial and novel sorbents under environmentally relevant conditions as described below.

2.2 Synthesis of library of 1st generation ionic fluorogels

Chemical stability of ionic fluorogels was achieved by end-functionalization of PFPEs with polymerizable functionality connected through aryl-ether linkages. Copolymerization of these PFPEs with an amine-containing monomer resulted in a library of IFs with systematic variations of network architecture and cation density. In order to explore the influence of polymer network architecture, we identified two PFPE oligomers—Fluorolink® E10H (E10H) and fluorinated tetraethylene glycol (FTEG)—which have analogous chemical structures and different molecular weights (Figure 1A). Fluorolink® E10H has a similar molecular weight to the material used in our previous study (~1,600 g/mol) (Kumarasamy et al., 2020) while FTEG is a short PFPE oligomer (410 g/mol). Nucleophilic aromatic substitution of pentafluorostyrene (PFS) using the hydroxy end groups of the PFPEs (Figure 1A) yielded PFS-capped oligomers of E10H and FTEG. The same nucleophilic aromatic substitution approach was used to synthesize an amine-containing monomer **1** to ensure similar copolymerization kinetics between IF building blocks.

Synthesis of IF was achieved through the thermally initiated radical copolymerization of PFS-E10H, PFS-FTEG, and **1** (Figure 1B) to form polymer networks, which were subsequently quaternized with methyl iodide, crushed into granules, and sieved to isolate IF grains of a desired size. The range of IF compositions prepared is reported in Figure 2 and represents a library of materials that systematically vary the incorporation of fluorophilic and electrostatic components, as well as vary network architecture. The amine content of the IF was held constant at either 20 or 40 weight % amine comonomer, a range of amine incorporation that has provided efficient PFAS removal in previous studies (Kumarasamy et al., 2020).

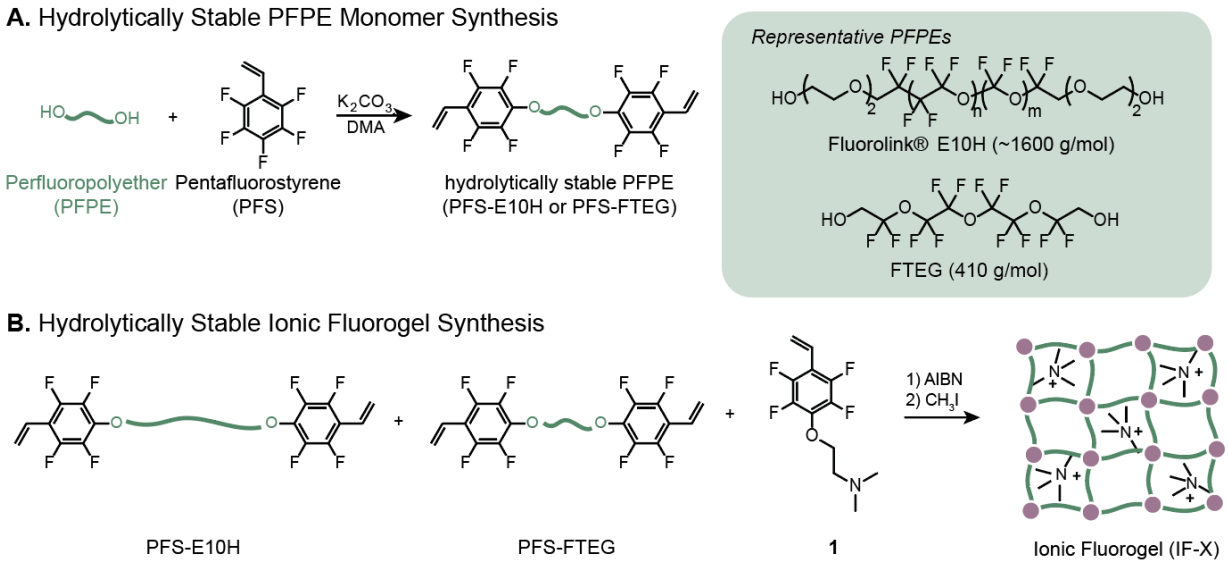

Figure 1. A. Synthesis of PFPE crosslinkers (PFPEs starting materials shown in shaded inset). **B.** Synthesis of Ionic Fluorogel formulations (denoted as IF-X), with varied compositions of PFS-E10H, PFS-FTEG, and **1**. Resulting crosslinked materials after polymerization were ground and sieved to obtain resin particles 75-125 mm.

Library of Ionic Fluorogels

	Reference	IF-1	IF-2	IF-3	IF-4	IF-5	IF-6	IF-7	IF-8	IF-9	IF-10
wt % comonomer	PFS-E10H	80	60	40	20	0	60	50	30	10	0
	PFS-FTEG	0	20	40	60	80	0	10	30	50	60
	1	20	20	20	20	20	40	40	40	40	40
	T_g (°C)[a]	10	6.6	5.9	9.1	3.7	11	17	10	12	14
	Swelling Ratio[b]	1.3	1.4	1.5	1.2	1.2	1.6	1.5	1.2	1.3	1.1

Figure 2. Library of 1st generation Ionic Fluorogels. [a] Calculated by Differential Scanning Calorimetry during the second heating cycle at a rate of 10 °C/min. [b] Ratio of swollen to dry mass of IF after swelling in 0.1 M NaCl.

2.3 Synthesis of 2nd generation ionic Fluorogels

Commercial fluoroolefin-vinyl ether (FVE) copolymer (1 eq., 200 mg) was dissolved in 2-methyltetrahydrofuran (0.3M), and added to and 8 mL glass vial containing multiamine (varied equivalents), sodium iodide (1 eq., 118 mg), Hunig's base (1 eq., 102 mg). The reaction mixture was sparged under N_2 for 10 minutes, then sealed with the vial cap and electrical tape. The mixture was then heated to 75 °C over 24 hours with no stirring. After an insoluble gel was

formed, the crude product was removed from heat, ground into multiple pieces, and purified via Soxhlet extraction with ethanol. IF 2-X was then dried in a vacuum oven at 50 ^{o}C to yield the pure product as a brown powder. The resulting powder was ground and sieved to between 75-125 microns for evaluation in batch and column tests.

2.4 Characterization of ionic fluorogels

Ionic fluorogels were characterized for their swelling ratio, thermal behavior, and mechanical properties. To evaluate the swelling ratio photocured discs of IF were swollen in deionized water for 24 hours, massed, then dried under vacuum and massed again. The swelling ratio was calculated as the mass of swollen resin divided by the mass of dry resin. This analysis was completed in triplicate for each IF formulation. Thermal gravimetric analysis (TGA) was performed on a TA Instruments TGA (Discovery Series) using 5-8 mg of the sample. The samples were heated to 25-600 °C at a temperature ramp rate of 10 °C/min. Infrared (IR) spectra were obtained using PerkinElmer Frontier FT-IR spectrometer. Differential scanning calorimetry (DSC) was performed on a TA Instruments Discovery DSC. T_g values were determined from the second heating scan. All experiments were run at a ramp rate of 10 ^{o}C/min. Mechanical analysis was performed via dynamic Oscillatory rheology on a TA Instruments Discovery HR-3 Rheometer using an 8mm Aluminum Peltier Plate. Experiments were run at 25 ^{o}C at 1.0 % strain from 0.1 to 500 rad/s to obtain the elastic modulus (G') and loss modulus (G'') as a function of frequency.

2.5 Water sample analysis with LCMS for PFAS evaluation

Water samples were stored under refrigeration until analysis. A 180 µL aliquot of sample and 20 µL of stable isotope-labeled analogues (Wellington Labs, Guelph, CA, product numbers MPFAC-C-ES and M3HFPO-DA) were transferred to polypropylene autosampler vials and closed with caps fitted with silicone septa. No other processing was done as per a direct injection method by (Sun et al., 2016).

Analysis of target compounds PFOA, PFHxA, and GenX was performed using an Accela HPLC system coupled to a TSQ-Quantum Ultra triple-quadrupole mass analyzer (Thermo Scientific, San Jose, CA) operated in negative ion mode. Analytes were separated on a 2.1 × 50 mm Sunfire C18 3.5 µm column (Waters Corporation, Milford, MA) with gradient elution at a flow rate of 350 µL per min. Binary mobile phase consisted of 95:5:water:methanol containing 2 mM ammonium acetate (A) and 5:95:water:methanol containing 2 mM ammonium acetate (B). Composition started at 25% B, was held for 0.5 min, increased linearly to 90% B over 2 min, was held at 90% B for 1.5 min, decreased linearly to 25% B over 0.1 min, and held at 25% B for 0.9

min for column equilibration. Mass spectrometer parameters were as follows: spray voltage of 3000 V, vaporizer temperature of 150 ^{o}C, sheath gas flow rate 40, auxiliary gas flow rate 20, capillary temperature of 225 ^{o}C, argon collision gas pressure of 1.0 mTorr, 0.05 sec per scan, quadrupole 1 resolution of 0.5 amu, quadrupole 3 resolution of 0.7 amu and collision energy 10 eV. Linear or quadratic calibration curves using the analyte to internal standard ratio were used to calculate analyte amounts. Calibration points were 2, 10, 50, 200, and 1000 pg analyte versus 200 pg internal standard for PFCAs and PFASs.

Additional details about PFAS analysis, including analysis of 21 PFAS and nontargeted analysis can be found in Appendix 3. The tabulated analyte-specific information including mass transitions is reproduced in Table 1 (also available in Appendix 3).

Table 1. List of Target PFAS Analytes.

Analyte	Acronym	CAS #	Exact Mass (g/mol)	Acquisition Window (min)	MS/MS Transition (*m/z*)	Collision Energy (V)	Min Dwell Time (ms)	RF Lens (V)	Internal Standard	Detection Limit (pg on column)
Perfluoroalkylcarboxylic Acids (PFCA)										
Perfluorobutanoic acid	PFBA	375-22-4	213.9865	0 - 4.0	213 → 169	8.66	16.306	59	M4PFBA	2
Perfluoropentanoic acid	PFPeA	2706-90-3	263.9833	3.8 - 5.2	263 → 219	7.91	2.719	65	M5PFPeA	0.5
Perfluorohexanoic acid	PFHxA	307-24-4	313.9801	4.5 - 5.7	313 → 269	8.37	2.719	75	M5PFHxA	0.25
Perfluoroheptanoic acid	PFHpA	375-85-9	363.9769	4.7 - 5.7	363 → 169 363 → 319	16.54 8.71	2.719	84	M4PFHpA	0.1
Perfluorooctanoic acid	PFOA	335-67-1	413.9737	5.0 - 6.0	413 → 169 413 → 369	17.26 9.25	2.719	91	M8PFOA	0.5
Perfluorononanoic acid	PFNA	375-95-1	463.9705	5.1 - 6.1	463 → 219 463 → 419	15.95 9.68	2.719	103	M9PFNA	1
Perfluorodecanoic acid	PFDA	335-76-2	513.9673	5.3 - 6.3	513 → 269 513 → 469	16.88 10.14	3.155	109	M6PFDA	0.25
Perfluoroalkylsulfonates (PFSA)										
Potassium perfluorobutanesulfonate	PFBS	29420-49-3	337.9062	4.5 - 5.5	299 → 80 299 → 99	32.67 28.88	2.719	168	M3PFBS	0.5
Sodium perfluorohexanesulfonate	PFHxS	82382-12-5	421.9258	5.0 - 6.0	399 → 80 399 → 99	37.31 34.78	2.719	222	M3PFHxS	1
Sodium perfluorooctanesulfonate	PFOS	4021-47-0	521.9194	5.1 - 6.5	499 → 80 499 → 99	41.18 40.55	2.719	299	M8PFOS	2
Perfluoroalkyl Ether Acids (PFEA)										

Difluoro(perfluoromethoxy)acetic acid	PFMOAA	674-13-5	179.9846	0 - 4.0	179 → 85	10.39	16.306	65	MPFBA	0.25
Perfluoro-2-(perfluoromethoxy)propanoic acid	PMPA	13140-29-9	229.9814	0.8 - 4.5	185 → 85 185 → 119	14.56 9.76	14.96	68	MPFBA	2
Perfluoro-3,5-dioxahexanoic acid	PFO2HxA	39492-88-1	245.9763	3.7 - 5.1	201 → 85 201 → 135	13.3 9.04	3.817	70	M5PFPeA	1
1,1,2,2-Tetrafluoro-2-(1,2,2,2-tetrafluoroethoxy)ethane-1-sulfonic acid	NVHOS	801209-99-4	297.9546	4.0 - 5.3	297 → 80 297 → 135	34.82 26.27	2.719	170	M5PFPeA	1
2,3,3,3-Tetrafluoro-2-(pentafluoroethoxy)propanoic acid	PEPA	267239-61-2	279.9782	4.0 - 5.3	235 → 119 235 → 135	8.96 15.19	2.719	71	M5PFPeA	0.25
Perfluoro-3,5,7-trioxaoctanoic acid	PFO3OA	39492-89-2	311.9680	4.6 - 5.6	311 → 85 311 → 151	10.9 5.25	2.719	49	M5PFHxA	0.5
Perfluoro-2-methyl-3-oxahexanoic acid	HFPO-DA or GenX	13252-13-6	329.9750	4.6 - 5.6	285 → 169 285 → 185	5.34 16.92	2.719	48	M5PFHxA	1
Perfluoro-3,5,7,9-butaoxadecanoic acid	PFO4DA	39492-90-5	377.9597	4.9 - 5.9	377 → 85 377 → 151	11.36 5.25	2.719	58	M8PFOA	2
2,2,3,3-Tetrafluoro-3-{[1,1,1,2,3,3-hexafluoro-3-(1,2,2,2-tetrafluoroethoxy)propan-2-yl]oxy}propanoic acid	HydroEve	773804-62-9	427.9730	4.9 - 5.9	427 → 283	11.7	2.719	106	M8PFOA	0.5
1,1,2,2-Tetrafluoro-2-{[1,1,1,2,3,3-hexafluoro-3-(1,2,2,2-tetrafluoroethoxy)propan-2-yl]oxy}ethane-1-sulfonic acid	Nafion Byproduct 2	749836-20-2	463.9399	5.1 - 6.1	463 → 263	26.95	2.719	168	M9PFNA	0.1
Perfluoro-3,5,7,9,11-pentaoxadodecanoic acid	PFO5DA	39492-91-6	443.9515	5.1 - 6.1	443 → 85 443 → 151	12.88 5.25	2.719	75	M9PFNA	1
Internal Standards										
Perfluoro-n-[$^{13}C_4$]butanoic acid	M4PFBA	n/a	218.0001	0 - 4.0	217 → 172	8.75	16.306	60	n/a	n/a

Perfluoro-n-[$^{13}C_5$]pentanoic acid	M5PFPeA	n/a	269.0003	3.8 - 5.2	268 → 223	8.12	2.719	69	n/a	n/a
Sodium perfluoro-1-[2,3,4-$^{13}C_3$]butanesulfonate	M3PFBS	n/a	324.9424	4.5 - 5.5	302 → 80 302 → 99	32.3 29.09	2.719	165	n/a	n/a
Perfluoro-n-[1,2,3,4,6-$^{13}C_5$]hexanoic acid	M5PFHxA	n/a	318.9971	4.5 - 5.7	318 → 273	8.41	2.719	74	n/a	n/a
Perfluoro-n-[1,2,3,4-$^{13}C_4$]heptanoic acid	M4PFHpA	n/a	367.9905	4.7 - 5.7	367 → 322	8.92	2.719	86	n/a	n/a
Perfluoro-n-[$^{13}C_8$]octanoic acid	M8PFOA	n/a	422.0009	5.0 - 6.0	421 → 376	9.42	2.719	95	n/a	n/a
Sodium perfluoro-1-[1,2,3-$^{13}C_3$]hexanesulfonate	M3PFHxS	n/a	424.9360	5.0 - 6.0	402 → 80 402 → 99	36.84 35.2	2.719	225	n/a	n/a
Perfluoro-n-[$^{13}C_9$]nonanoic acid	M9PFNA	n/a	473.0011	5.1 - 6.1	472 → 427	9.59	2.719	105	n/a	n/a
Perfluoro-n-[1,2,3,4,5,6-$^{13}C_6$]decanoic acid	M6PFDA	n/a	519.9877	5.3 - 6.3	519 → 474	10.05	3.155	114	n/a	n/a
Sodium perfluoro-1-[$^{13}C_8$]octanesulfonate	M8PFOS	n/a	529.9466	5.1 - 6.5	507 → 80 507 → 99	41.39 41.23	2.719	299	n/a	n/a

2.6 Evaluation of sorption of PFAS in laboratory waters

2.6.1 Overview

A variety of tests were performed to evaluate sorption of PFAS in laboratory waters. This included batch sorption of three representative PFAS (PFOA, PFHxA and GenX), binding isotherm studies, and GenX sorption kinetics tests. For each of these tests, control experiments to account for PFAS losses during handling were performed under identical conditions in the absence of sorbent. Experiments were performed in triplicate.

2.6.2 Batch sorption of PFAS in laboratory water

Batch adsorption studies of mixtures of PFAS (PFOA, PFHxA and GenX) were performed in a 1-L polypropylene bottle equipped with a magnetic stir bar (700 rpm) at room temperature. The test solution consisted of 1 L of deionized water with 200 mg/L sodium chloride, 20 mg/L of humic acid (Sigma-Aldrich®, Saint Louis, MO), 10 mg/L of ionic fluorogel, and 1 μg/L of each PFAS. Water samples (10 mL) for evaluation of PFAS removal were withdrawn at 21 h of absorption time, and filtered through either 0.2 μm PTFE or 0.45 μm cellulose acetate filter. The first 5 mL was drained to avoid any electrostatic effect from the filter and the remaining 5 mL was collected for LCMS analysis. The percent PFAS removal (%PFAS removal) by sorbents was determined as given by

$$\% \text{ PFAS removal} = \frac{C_0 - C_t}{C_0} \times 100$$

C_0 (mg L^{-1}) = Initial concentration of PFAS
C_t (mg L^{-1}) = Residual concentration of PFAS

2.6.3 Binding isotherm studies

Batch isotherm studies were performed in 125 mL polypropylene bottle (100 mL operating volume) equipped with a magnetic stir bar (500 rpm) at 23-25 °C. The test solution consisted of deionized water dosed with 100 mg/L of ionic fluorogel and GenX spiked to initial concentrations of 0.2, 1, 5, 10, 20, 30 and 50 mg/L. Water samples for evaluation of PFAS removal were withdrawn at 21 h of absorption time, centrifuged for 15 minutes, and the supernatant from the top was taken for LCMS analysis. High concentration samples were serially diluted (5-10 mg/L diluted 20x and 20-50 mg diluted 100x) before LCMS analysis. Sorption data was fitted to Langmuir and Freundlich sorption isotherms.

2.6.4 GenX sorption kinetics

The kinetics of sorption of GenX were evaluated in 125 mL polypropylene bottles equipped with a magnetic stir bar (500 rpm) at room temperature. The test solution (100 mL) contained a sorbent dose of 10 mg/L and GenX concentration of 200 μg/L or 1 μg/L. About 1 mL aliquot was taken at each predetermined time intervals (0.5, 1, 5, 10, 30, 60, mins and 21, 48 and 72 h), centrifuged for 15 minutes, and the supernatant analyzed by LCMS to determine the residual GenX concentration.

2.7 Evaluation of sorption of PFAS in natural water

2.7.1 Overview

Two sets of tests were performed to evaluate sorption of PFAS in laboratory natural waters. This included batch sorption tests and flow-through, packed-bed sorption tests using representative PFAS. For each of these tests, control experiments to account for PFAS losses during handling were performed under identical conditions in the absence of sorbent. Reference sorbents (i.e., commercial IX resins and GAC) were also evaluated.

2.7.2 First Generation Materials – batch sorption of 21 PFAS in settled conventional water

Sorption tests with settled conventional water (OWASA, Chapel Hill, NC, pH = 5.34, TOC ≤ 0.5 mg/L, conductivity 180 μS/cm) spiked with 21 PFAS ($[PFAS]_0$ = 1 ug/L each) (Table 1) were performed at room temperature in 100mL polypropylene bottles equipped with a magnetic stir bar. A 2 mL aliquot was taken immediately before adding 10 mg IF-1 and at time = 30, 60, 120, 240 minutes and 24 hours. The aliquots were filtered through a 0.45 um cellulose acetate syringe filter, then centrifuged 5 minutes. 1mL of supernatant was transferred to a clean 1.5-mL snap-top tube, then analyzed by LCMS to determine the residual PFAS concentration. Controls were performed with either no PFAS, or no PFAS and no resin.

2.7.3 First Generation Materials – flow-through, packed-bed sorption of 21 PFAS in settled conventional water

Filtered settled conventional water was spiked with PFHxA, PFOA, and GenX, each at a concentration of ~500 ng/L, and exposed to air at ambient temperature (~22 ^{o}C) overnight. Bench-scale RSSCT experiments were performed in accordance with the protocols stipulated in ASTM 6586-03 (ASTM International, 2021). The respective RSSCT columns were scaled from a

representative pilot-scale column based on the constant diffusivity (CD) similitude approach (see additional details in Appendix 3). This scaling approach has been validated for PFAS sorption via GAC (Park et al., 2020; Zeng et al., 2020; Najm et al., 2021) and IX (Schaefer et al., 2019; Zeng et al., 2020) from PFAS-impacted waters with low levels of dissolved organic carbon, which is synonymous with the type of water used in this study. Columns were made of polypropylene (PP) with an inner diameter of 0.318 cm (Grainger, Lake Forest, IL). Granular sorbents were pulverized and sieved with mesh sizes of #200 and #230 to obtain a desired mean particle diameter of 0.0685 mm. The sorbent was loaded as a slurry into the column (1.35 cm bed depth) between two wetted pieces of glass wool (0.008 mm diameter, Fisher Scientific). The hydraulic loading rate (HLR) and empty bed contact time (EBCT) of the RSSCT were 26.3 m/h and 0.03 min, respectively, and were calculated assuming a HLR and EBCT of 36.7 m/h and 3 min, respectively, for the representative pilot-scale column. Effluent samples were collected in PP centrifuge tubes at predetermined intervals and stored at 4^{o}C prior to analysis. Experiments were performed in duplicate through ~150,000 bed volumes (BVs).

2.7.4 Second Generation Materials – batch sorption experiments

Sorption tests were conducted at room temperature in 500 mL rectangular polypropylene bottles equipped with a magnetic stir bar. Water was filtered through a 1 µm filter and spiked with PFOA, PFHxA, GenX, and PFMOAA ($[PFAS]_0$ = 1 ug/L each). IFs, GAC, and commercial IX were dosed to each bottle at 20 mg/L and stirred at 700 rpm. After 21 hours, stirring was stopped and sorbents were allowed to settle for 5 minutes before the supernatant was collected and filtered through a 0.22 µm filter. All experimental conditions were tested in duplicate. Controls were performed with PFAS and no resin dosed. Tests were conducted using the waters listed below, with water quality included in Table 2.

- OWASA Jones Ferry WTP settled conventional water
- Greensboro Mitchell WTP settled conventional water
- Cape Fear Public Utility Authority (CFPUA) Sweeney WTP settled conventional water
- CPFUA Well P raw water (feed well for the Richardson WTP)
- East Burlington WWTP effluent

Table 2. Source Water Quality.

Water Source	TOC mg/L	Cl^- mg/L	SO_4^{2-} mg/L	NO_3^- mg/L
OWASA Jones Ferry WTP Settled	1.4	6	50	2
City of Greensboro Mitchell WTP Settled	1.5	7	26	1
CFPUA Sweeney WTP Settled	1.8	14	36	4
CPFUA Well P	2.1	22	9	ND
City of Burlington East Burlington WWTP Effluent	13.4	53	48	47

2.7.5 Second Generation Materials – flow-through, packed-bed sorption

RSSCTs for the 2nd generation materials were conducted under similar conditions to those for the 1st generation materials, with a few modifications. For column depth, IF and IX materials were tested at 1.5 cm depth and scaled to a 2 min EBCT. GAC materials were tested at 3.5 cm column depth and scaled to a 7.5 min EBCT. IF, IX, and GAC materials were tested in singlet to ~370,000 BV, ~375,000 BV, and ~145,000 BV, respectively. Mean particle diameters for IF, IX, and GAC were 68.5 μm, 97 μm, and 89 μm, respectively. Water used for these tests were not spiked with PFAS.

2.8 Ionic fluorogel regeneration tests

Five cycles of sorption and desorption of GenX with IF-1 were performed to assess the regenerability of IFs and performance after regeneration. To perform these tests, a small packed-bed of IF-1 (20 mg) was created in a 0.45 μm PTFE filter (25 mm) via filtration of a 400mM ammonium acetate in 1:1 EtOH:H_2O (20 mL) solution containing the fluorogel followed by filtration of deionized water, if needed. The absorption stages consisted of filtration of a solution of GenX (18 mg/L, 20 mL) through the filter over 2 mins. To remove any trace of GenX solution in the filter before the desorption stage, the filter was washed by passing through deionized water (20 mL). The desorption stage consisted of passing through the filter 20 mL of a 1:1 EtOH:H2O solution containing 400 mM ammonium acetate over 2 minutes. The GenX concentration in the effluent was evaluated by LCMS in both the sorption and desorption stages. Before the next absorption stage, the filter was washed by passing through deionized water (20 mL) to remove any trace of methanolic solution left over and the residual deionized water was removed by vacuum suction.

2.9 Ionic fluorogel stability tests

The stability of pre-weighed IF-1 and IF-20+ (Kumarasamy et al., 2020) photocured discs after exposure to alkaline solutions was evaluated. The discs were pre-weighed and suspended in 2 mL alkaline solution for a defined period (i.e., 1, 2, 4, and 8 weeks), then removed from the suspension. After removal, the discs were washed once with deionized H_2O, massed, dried, soaked in 400 mM methanolic ammonium acetate solution over 2hr, washed with deionized H_2O, dried, and massed again. Alkaline solutions consisted of a glycine-$NaHCO_3$ buffer (pH 8.7) and a $NaHCO_3$-NaOH buffer (pH 11.7). Exposure to alkaline solution was performed in an incubator at either 23 ^oC or 50 ^oC. Swelling ratio was determined by the ratio of swollen to dried mass before washing with MeOH solution. Percent mass loss was determined from the initial and final (after MeOH wash) dry mass. The degradation media were submitted for nontargeted analysis to determine if any PFAS were leached upon resin degradation. Each experiment was run in triplicate.

3. Results and Discussion

3.1 Physical properties and stability of 1st generation ionic fluorogels

A library of IFs was synthesized with the PFS-capped oligomers of EH10H and FTEG which have analogous chemical structures and different molecular weights (Figure 1A). The range of IFs compositions used is summarized in Figure 2 along with the measured glass transition temperatures (T_g) and swelling ratios. The resulting materials were elastomers with low swelling ratios (1.1-1.6) in 0.1M NaCl. Notably, the swelling ratio was generally higher for materials with higher incorporation of ammonium ion, which is presumably due to both increased hydrophilicity and decreased crosslink density. The T_g of the IFs did not change considerably with the subtle differences in chemical composition and remained between 3.7 and 14 ^oC. Light and scanning electron microscopy images of the materials (Figure 3) demonstrated their granular nature and lack of appreciable porosity.

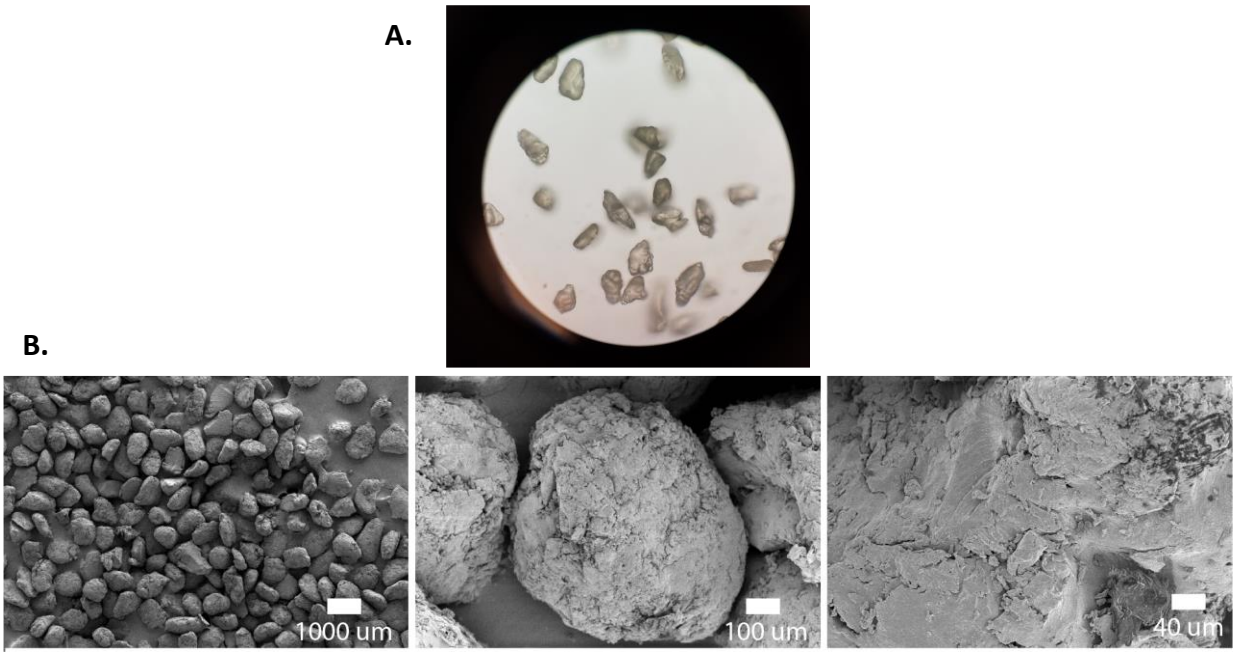

Figure 3. (A) Light microscope image at 100x magnification of IF-8 showing the granular nature of the resin. (**B)** SEM images of IF-8 at 2.0 kV.

We fabricated structurally tunable and chemically stable IF resins. Chemical stability was achieved by end-functionalization of PFPEs with polymerizable functionality connected through aryl-ether linkages. This contrasts with our previous generation IF resins (Kumarasamy et al., 2020) which contain ester and carbamate linkages that we hypothesized would degrade significantly over time in aqueous solution. We performed accelerated degradation studies (i.e., immersion in basic solution at pH 8.7 at 50 ^{o}C for up to 56 days) with IF-1 (Figure 2) and the structurally similar IF-20+ from the previous generation IF resins (Kumarasamy et al., 2020). The hydrolytically stable IF-1 maintained a low swelling ratio and consistent mass, while the IF-20+ with ester and carbamate linkages degraded significantly, suffered precipitous loss and 38% mass loss over 56 days (Figure 4A).

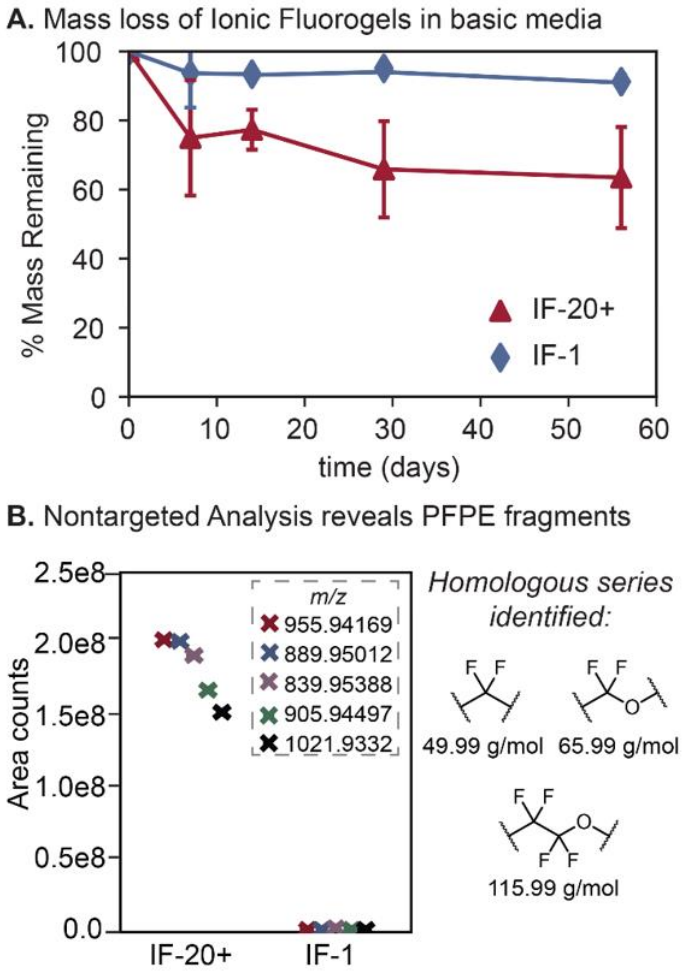

Figure 4. (A) Mass loss of IF-20+ (red triangles) and IF-1 (blue diamonds) over 56 days. pH = 8.7, 50 ^{o}C. Error bars: standard deviation of 3 experiments. Discs were washed with methanol before drying to determine mass loss. **(B)** Averaged area counts (duplicate samples) of the 5 most-intense peaks detected via nontargeted analysis of the extracts after washing the samples from day 28 of the mass loss study in methanol. The *m/z* values vary by combinations of 49.99, 65.99, and 115.99, indicative of PFPE repeat units.

To identify the degradation products of IF hydrolysis, nontargeted analysis via high-resolution mass spectrometry was used to analyze the aqueous media and methanol extracts isolated from each degradation time point (McCord et al., 2020; Washington et al., 2020). The nontargeted analysis of IF-20+ revealed characteristic homologous series of *m/z* values for PFPEs in the IF-20+ methanol extract (Figure 4B). The five *m/z* values with the highest area counts via MS vary by approximately 49.99, 65.99 or 115.99, characteristic of the difluoromethylene (CF_2), difluoromethylene glycol (CF_2O), and tetrafluoroethylene glycol (CF_2CF_2O) (Figure 4B) repeat units present within Fluorolink® PFPEs (McCord et al., 2020; Washington et al., 2020). Minimal peak areas were observed for the same *m/z* values in the aqueous IF-20+ degradation media,

indicating that degraded fluoropolymer remained trapped in the IF matrix until desorption with organic solvent (Figure 5). In contrast, nontargeted analysis of the aqueous media and methanol extracts of IF-1 demonstrated over two orders of magnitude lower area counts of characteristic PFPE peaks relative to IF-20+ (Figures 4b, 5). These data support the hypothesis that end-modification of PFPE oligomers with perfluorostyrene enables synthesis of more hydrolytically stable IFs.

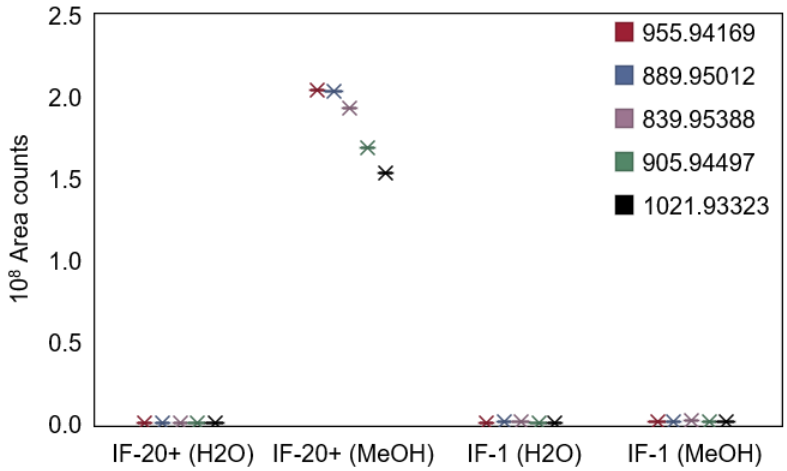

Figure 5. Comparison between averaged area counts of degradation media (H2O) and methanol extracts (MeOH) of IF-20+ and IF-1 subjected to nontargeted analysis. Duplicate samples.

3.2 Influence of polymer network architecture on PFAS removal

To explore the influence of polymer network architecture, we used the library of quaternized IFs summarized in Figure 2. The effect of network architecture on PFAS removal performance was evaluated through batch PFAS sorption experiments under simulated natural water conditions using PFOA (long-chain), PFHxA (short-chain), and GenX (branched) as target contaminants (Figure 6). Many IFs removed over 75% each of PFOA, PFHxA, and GenX, and all IFs outperformed Purolite 694AE, a commercial IX used for PFAS remediation. For example, IF-1, which had 20 wt% amine content and only the longer PFS-E10H as a fluorous component, had nearly complete PFOA removal and approximately 80% PFHxA and GenX removal. Varying network architecture had a marked effect on PFAS remediation. Specifically, IF-3, which contained the same ammonium content as IF-1 but contained 40 wt% of the shorter PFS-FTEG as a fluorous component, demonstrated enhanced performance for the remediation of the short-chain PFAS substrates PFHxA and GenX. Using only the shorter PFS-FTEG as a fluorous component (IF-5, IF-10), however, led to a decrease in performance compared to all the other materials. Further, the two best performing formulations (IF-3 and IF-8) had the same content of the longer

(PFS-E10H) and shorter (PFS-FTEG) fluorous components. From these data, we conclude that a heterogeneous distribution of mesh size within the polymer network improves PFAS sorption.

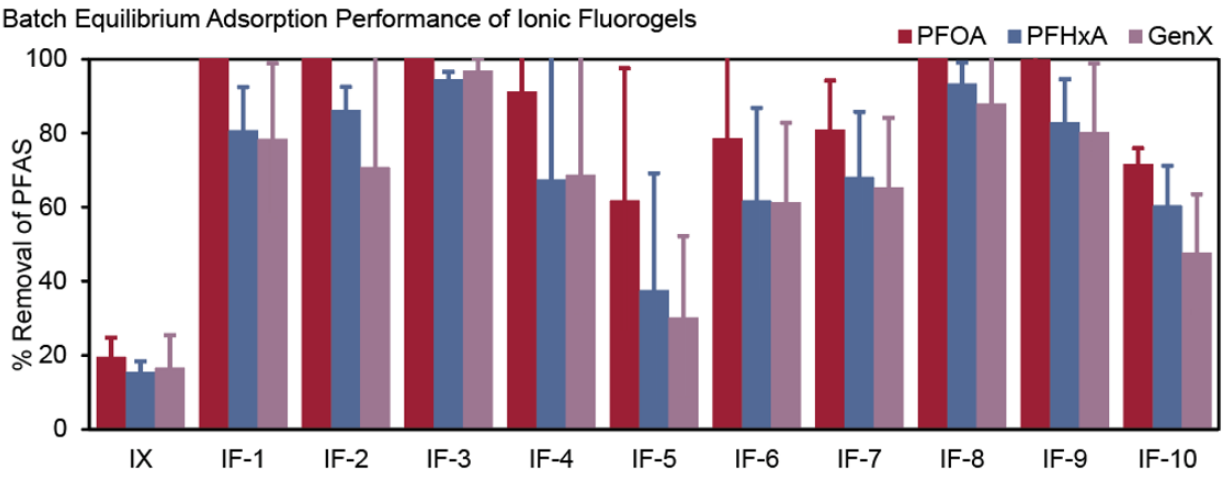

Figure 6. Batch equilibrium PFAS sorption by IFs. IX = Purolite 694AE. Water constituents: 200 mg/L NaCl and 20 mg/L humic acid; pH = 6.4; Sorbent: 10 mg/L; PFAS: (PFOA, PFHxA, GenX, 1 µg/L each); Equilibrium time: 21 h. Error bars: Standard deviation of 3 experiments. The composition of IF-1 through IF-10 is summarized in Figure 2.

3.3 Sorption kinetics and isotherm for GenX by 1st generation ionic fluorogels

We evaluated the sorption kinetics and isotherm for GenX, a model anionic PFAS, using IF-1, a high performing resin. IF-1 demonstrated rapid, irreversible adsorption of GenX in pure water reaching nearly maximum sorption within 1-2 h (Figure 7A). The IF-1 isotherm data demonstrated a better fit to the Langmuir model (R^2 = 0.96) relative to the Freundlich model (R^2 = 0.90) (Figure 7B), indicating that surface adsorption of GenX to the IF particle is likely the dominant method of PFAS removal from water (Swenson and Stadie, 2019). The Langmuir adsorption model indicated a binding capacity for GenX of 280 mg/g of resin, which is on par with the highest capacity for GenX in the literature at an environmentally relevant pH (278/mg/g) (Kumarasamy et al., 2020).

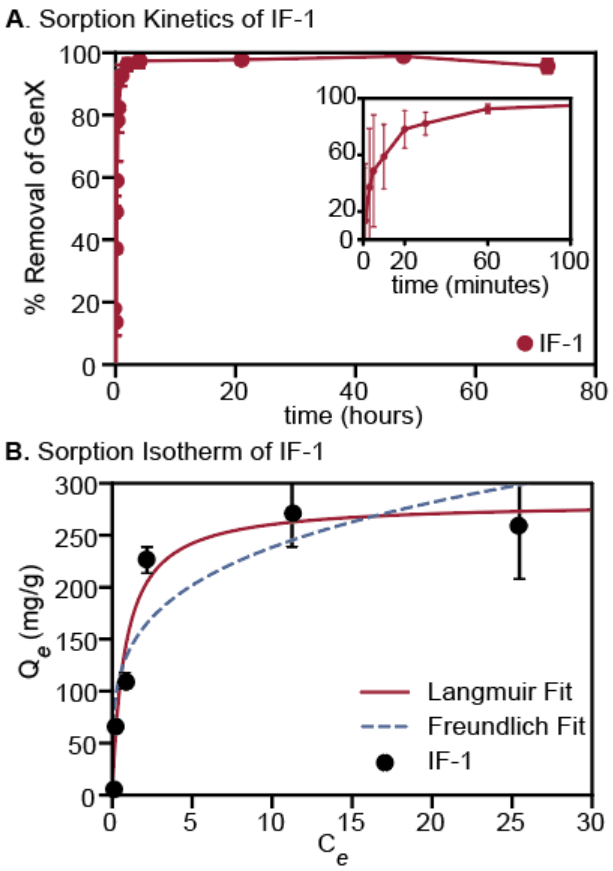

Figure 7. (A) Time dependent GenX sorption by IF-1 at $[GenX]_0$ = 1 µg/L; [IF-1] = 10 mg/L) concentration. pH = 9.7. Similar fast kinetics were obtained at $[GenX]_0$ = 1 µg/L (Appendix 3). **(B)** GenX Sorption Isotherm by IF-1 ([IF-1] = 100 mg/L; $[GenX]_0$ = 0.2-50 mg/L). Lines show fit to Langmuir (red, solid) and Freundlich (blue, dashed) models. Langmuir model: R^2 = 0.96; equilibrium constant K_L = 1.2 ± 0.5 L/mg; maximum sorption capacity at equilibrium Q_m = 280 ± 20 mg/g. Freundlich model: R^2 = 0.90; Freundlich constant K_F = 140 ± 20 mg/g)(L/mg)$^{1/n}$; intensity of adsorption *n* = 4.2.

3.4 Regenerability of 1st generation ionic fluorogels

The regenerability of IF-1 over multiple cycles of GenX sorption and desorption was investigated using a syringe filter containing IF-1. During loading of IF-1 with GenX, over 75% removal of GenX was achieved per LC-MS analysis of the filtrate, equivalent to 10-15 mg/g PFAS loading of the IF material. GenX was adsorbed and desorbed from IF-1 over 5 cycles (Figure 8) with no decrease in GenX sorption efficiency, using an environmentally friendly solvent (Capello et al., 2007). The ability to regenerate these IFs enables their reuse and creates a concentrated solution of PFAS that can be disposed of or destroyed through traditional or emerging technologies (Cui et al., 2020).

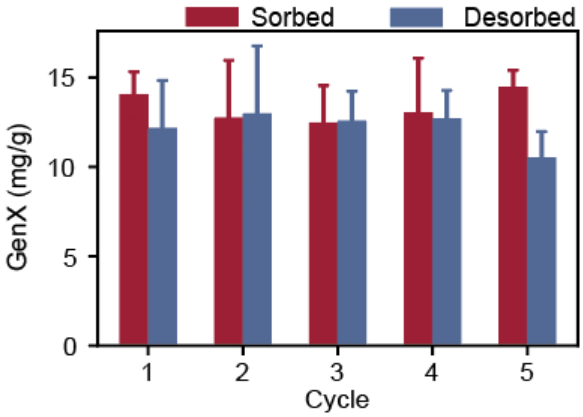

Figure 8. Regeneration and reuse over 5 cycles of IF-1. IF-1 = 20 mg, [GenX] = 18 mg/L (20 mL); extraction with 400 mM ammonium acetate in 1:1 EtOH:H_2O (20 mL). Error bars: Standard deviation of 3 experiments.

3.5 Synthesis of 2nd generation Ionic Fluorogels

Given the need for a scalable and chemically stable PFAS remediation technology, we next looked to other classes of partially fluorinated polymers which could serve as low cost, chemically stable, and high performance fluorophilic matrices for PFAS removal. To that end, we identified Fluoroolefin-Vinyl Ether copolymers (FVEs), a class of polymers with tunable fluorine density (from the fluoroolefin comonomer) and a wide variety of accessible functionality (from the vinyl ether comonomer).(Valade et al., 2009, 2010; Santhosh Kumar and Ameduri, 2010; Liu et al., 2011; Alaaeddine et al., 2012, 2013b, 2013a; Couture et al., 2013, 2015; Wang et al., 2013; Boschet and Ameduri, 2014; Hamiye et al., 2014; Dams and Hintzer, 2016; Lee et al., 2020; Mohammad et al., 2020) FVEs are attractive materials for a multitude of applications due to their resistance to chemical, thermal, and hydrolytic degradation, imparted by the high fluorine density and alternating structure of the polymer backbone.(Couture et al., 2011; Boschet and Ameduri, 2014; Li and Liao, 2017, 2018; Mohammad et al., 2020)

We hypothesized that FVEs would be excellent substrates for the development of new platform technology of chemically stable, versatile, and scalable 2nd generation IFs. The 2nd generation IFs comprise FVE copolymers that are chemically crosslinked into polymer networks through a nucleophilic displacement reaction with a reactive vinyl ether monomer. This platform allows the tuning the fluorophilicity of IFs by varying the fluoroolefin (tetrafluoroethylene, chlorotrifluoroethylene, hexafluoropropylene) and the vinyl ether (ethyl, *n*-butyl, *i*-butyl)

comonomers that comprise the FVEs. Additionally, commercially available FVEs may be leveraged as starting materials, highlighting the translational relevance of this method.

We hypothesized that tuning the identity of the nucleophile would impact PFAS sorption efficiency. To probe this tunability, we identified three representative nucleophiles (Figure 9). The first, Me6TREN, was a commercially available multiamine which we hypothesized we could leverage through nucleophilic substitution reactions with FVE copolymers to achieve IFs. The other two nucleophiles, multiamine 1 and multiamine 2, were aromatic-core trifunctional crosslinkers with varied functionality which we hypothesized would affect PFAS removal from water.

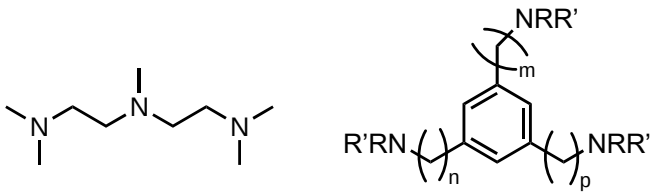

Me6TREN multiamine 1 multiamine 2

Figure 9. Representative multiamines used in synthesis of 2nd generation IFs.

We synthesized a systematic library of IFs (Table 3) by varying multiamine identity and weight percent incorporation, enabling systematic variation of crosslinking density and cation density. Representative synthesis of 2nd-generation IFs is shown for IF 2-1 in Figure 10. In a one-pot reaction, commercial FVE copolymer was dissolved in organic solvent, then multiamine crosslinker was added to the solution. Leaving groups on the FVE copolymer are substituted with the tertiary amines of Me6TREN, installing crosslinks and permanent cationic charge in a single step. The resulting granular materials were ground and sieved to between 75 and 125 microns for batch testing in various water sources.

Table 3. Library of 2nd generation IFs.

Entry	Multiamine	Weight % incorporation
IF 2-1	Me6TREN	20
IF 2-2	Multiamine 1	20
IF 2-3	Multiamine 1	30
IF 2-4	Multiamine 1	40
IF 2-5	Multiamine 2	20
IF 2-6	Multiamine 2	30
IF 2-7	Multiamine 2	40

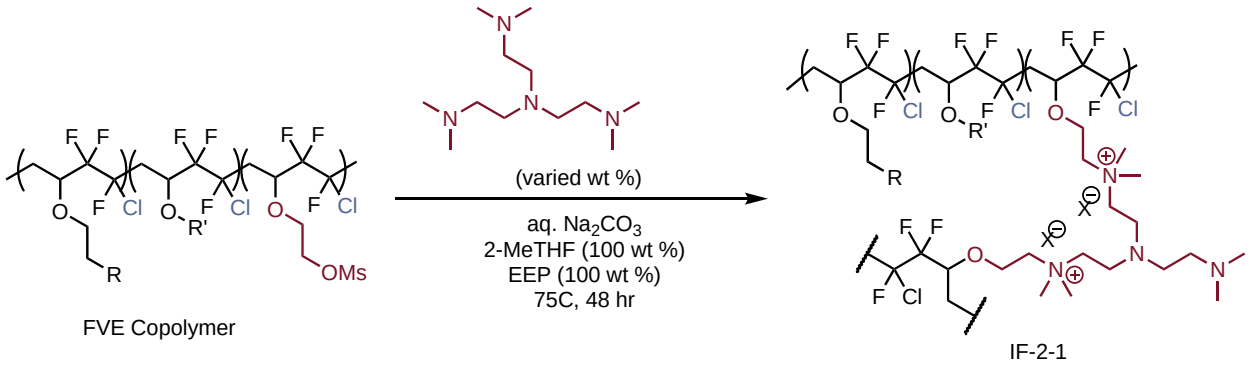

Figure 10. Representative 2nd generation IF synthesis (IF 2-1).

3.6 Batch results with lab water for 2nd generation ionic fluorogel

Initial screening of 2nd generation materials was achieved by subjecting each material to batch tests in pure water with sodium chloride added to it (Figure 11). Each sorbent was added at 10 mg/L loading and stirred for 3 hours. Then, PFAS solution (1ug/L each) was added, and the experiment was run for 21 hours before water sample collection for analysis by LC-MS relative to control samples without exposure to sorbents. Control experiments were also conducted using commercial anion exchange resins PFA694E and Purolite PSR2+.

Second generation IFs demonstrated a range of PFAS remediation efficiencies. IF 2-1, which leverages commercially available Me6TREN, demonstrated low to moderate removal efficiencies of most PFAS. However, IF 2-2 through 2-7 efficiently removed long-chain PFOA, PFOS, and PFNA, and were comparable to the two commercial resins. Short-chain PFAS removal was limited, however, compared to PSR2+, as well as compared to 1st generation materials subjected to the same experiment. These results highlight the difference that specific polymer

and crosslinker architectures may make; although the atomic composition of 1st and 2nd generation IFs are similar, the architecture and specific structure of 1st generation IFs likely enables them to outperform these 2nd generation materials.

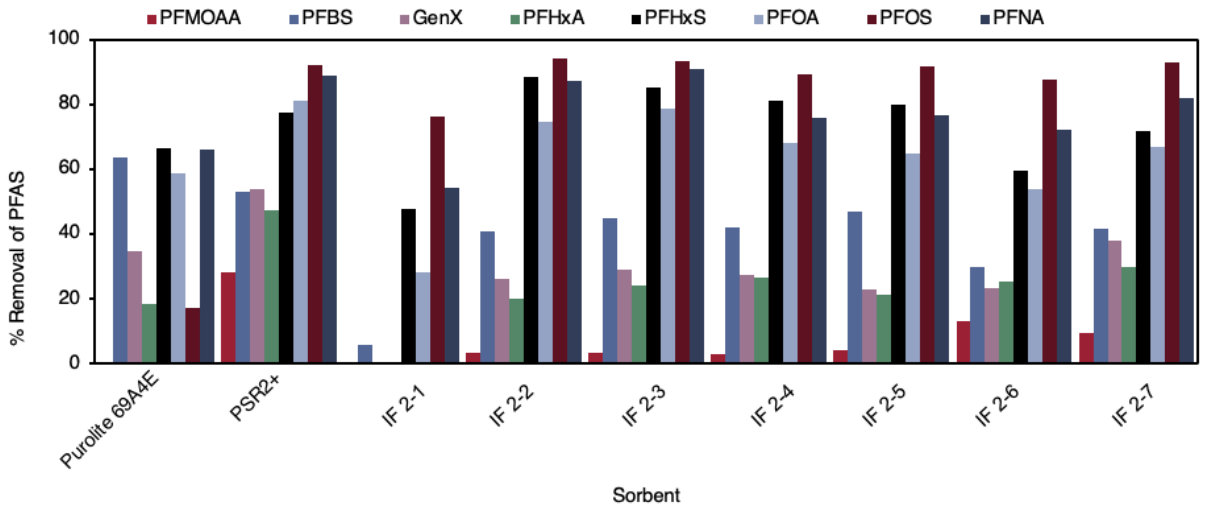

Figure 11. Batch equilibrium PFAS sorption by 2nd generation IFs. Water constituents: 200 mg/L NaCl; pH = 6.4; Sorbent: 10 mg/L; PFAS: (PFOA, PFHxA, GenX, 1 µg/L each); Equilibrium time: 21 h. Average of duplicate experiments shown. Meanings and acronyms of PFAS given in Table 1.

Despite the lesser performance of 2nd generation fluorogels compared with 1st generation fluorogels in batch tests, we hypothesize that tuning the synthesis and processing procedure for the 2nd generation IFs may improve PFAS removal performance. IF 2-6a (Figure 12) was synthesized as a variation of IF 2-6, wherein the crosslinker was formed *in situ* during the reaction. The resulting material demonstrated improved PFAS removal performance for seven of the eight analytes tested, indicating that we have not yet synthesized optimized materials from this class. Further research in this area to fine-tune the chemistry and synthesis procedure would be beneficial.

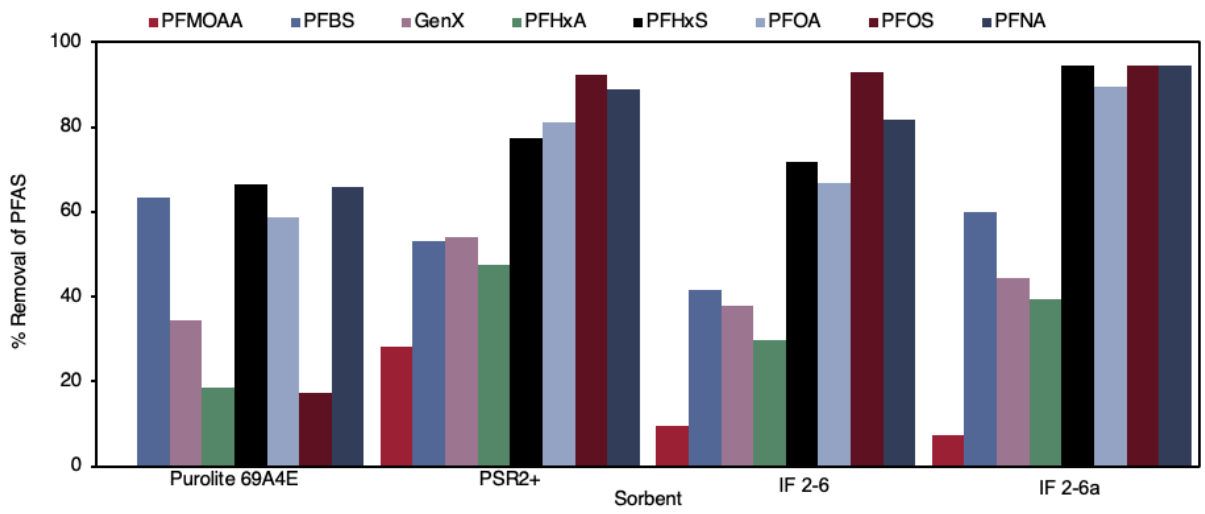

Figure 12. Batch equilibrium PFAS sorption by 2nd generation IF 2-6 and IF 2-6a relative to anion exchange resins. Water constituents: 200 mg/L NaCl; pH = 6.4; Sorbent: 10 mg/L; PFAS: (PFOA, PFHxA, GenX, 1 µg/L each); Equilibrium time: 21 h. Average of duplicate experiments shown. Meanings and acronyms of PFAS given in Table 1.

3.7 PFAS removal from natural water

3.7.1 Batch tests – 1st generation ionic fluorogels

We described in Section 3.2 (Figure 6) the removal of three representative PFAS (i.e., PFOA, PFHxA, and GenX) from simulated water by a range of structurally diverse and chemically stable IFs. The performance of the chemically stable IF-1 was also evaluated in batch tests using real water spiked with a chemically diverse mixture of PFAS at environmentally relevant concentrations (Figure 13). To that end, settled conventional (surface) water (pH = 5.34, TOC ≤ 0.50 mg/L, conductivity = 180 µS/cm) was spiked with 21 emerging and legacy PFAS at 1 µg/L each. Batch equilibrium adsorption of each PFAS using IF-1 (100 mg/L) resulted in greater than 77% removal for 18 of the 21 PFAS.

Closer analysis of this data elucidated the relationship between PFAS chemical structure and adsorption efficiency. Notably, analytes that contain only two (PFMOAA) or three (PFBA, PMPA, and PFO2HxA) perfluorocarbons, respectively, demonstrate less selective removal efficiency, which we hypothesize is due to their limited fluorophilic interaction with the IF resin. PFAS with four perfluorocarbons (PFPeA, PFBS, PEPA, PFO3OA, NVHOS) demonstrated 87 to 97% removal, and legacy PFAS with seven perfluorocarbons (PFOA) demonstrated over 98% removal. Additionally, these data demonstrate clear trends wherein perfluorinated sulfonic acids are

adsorbed more efficiently than their perfluorinated carboxylic acid counterparts, and linear PFAS are adsorbed more efficiently than their branched counterparts. These analyte structure–adsorption relationships align with our previous work (Kumarasamy et al., 2020) and provide more detailed support for our proposed mechanism of PFAS adsorption.

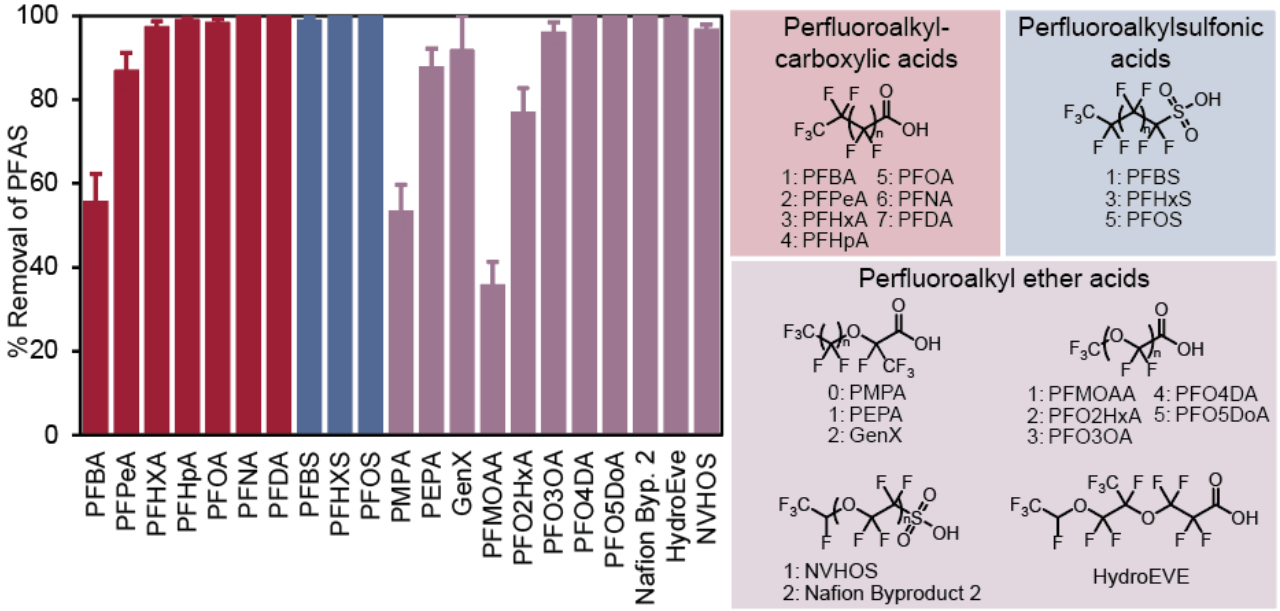

Figure 13. Batch equilibrium adsorption of 21 PFAS by IF-1 (100 mg/L). $[PFAS]_0$ = 1 µg/L each. Settled conventional water, OWASA, Chapel Hill, NC. Experiment time: 24 hours. Error bars: Standard deviation of 3 experiments. Meanings of acronyms for PFAS are listed in Table 1.

3.7.2 Batch tests – 2nd generation ionic fluorogels

Percent removal of different PFAS compounds for IF 2-3, IF 2-7, and PSR2+ are shown in Figure 14. PSR2+ outperformed both new IF formulations in all water matrices, whereas IF 2-7 was the better of the two IF formulations and demonstrated comparable removal (to PSR2+) of PFOA, PFHxA, and GenX in OWASA water. Both IFs exhibited their best performance in OWASA water, and did not perform as well in Greensboro and Sweeney waters. This is likely due to OWASA settled water having lower TOC (1.4 mg/L) compared to Sweeney (1.8 mg/L) and Richardson (2.1 mg/L).

Figure 15 shows PFAS removal by IF 2-3, a GAC product (Calgon F400), and PSR2+ grouped by different water types. IF 2-3 and PSR2+ generally outperformed GAC. Removals were highest in all waters for OWASA settled water, followed by CFPUA Well P. East Burlington WWTP effluent was the most challenging matrix tested, and only PSR2+ removed >50% of PFHxA and GenX in this matrix.

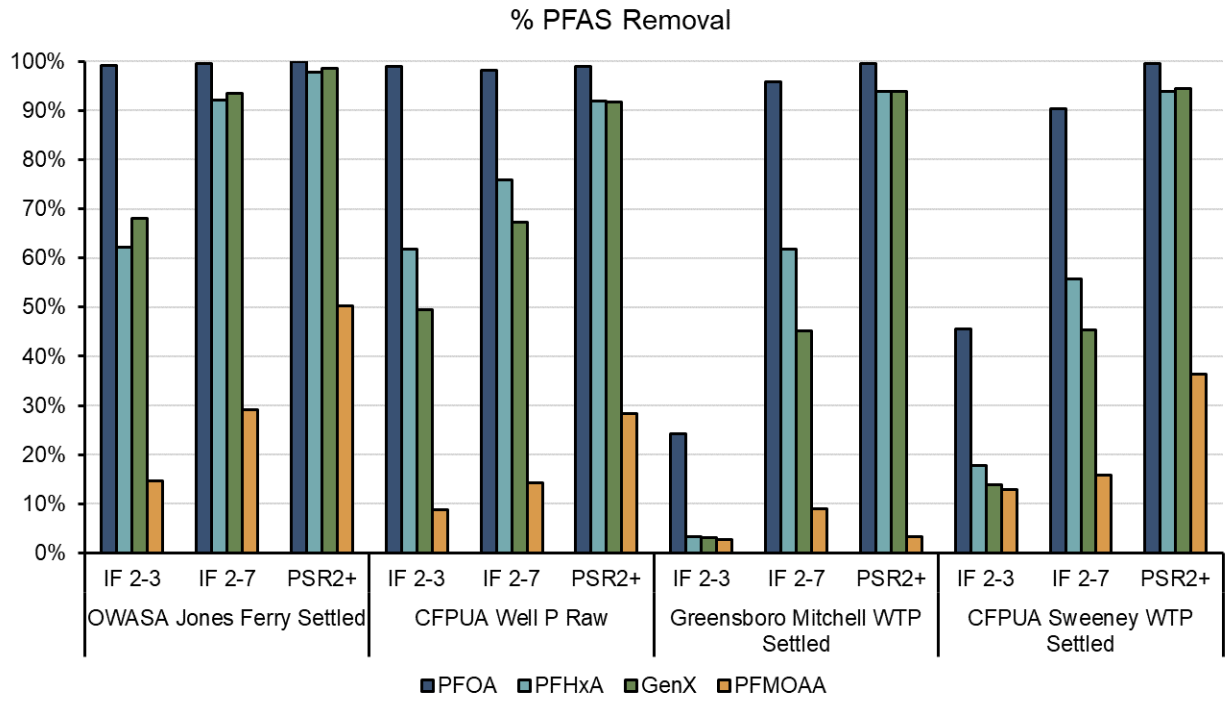

Figure 14. Comparison of 2nd generation IF with a commercial IX resin. $[PFAS]_0$ = 1µg/L each, sorbent dose = 20 mg/L. Experiment time: 21 hours. Meanings of acronyms for PFAS are listed in Table 1.

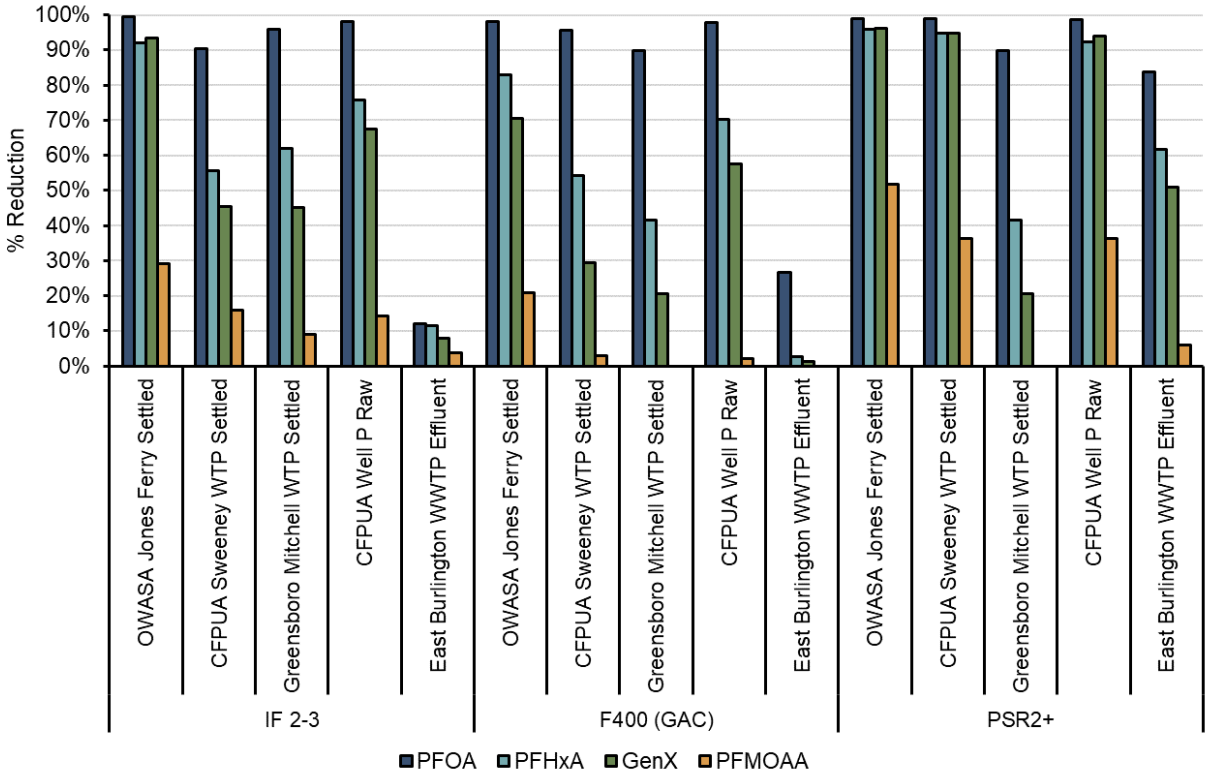

Figure 15. Efficacy of IF, GAC, and commercial IX across different natural waters. $[PFAS]_0$ = 1µg/L each, sorbent dose = 20 mg/L. Experiment time: 21 hours. Meanings of acronyms for PFAS are listed in Table 1.

3.7.3 Packed-bed tests – 1st generation ionic fluorogels

The most common mode of implementation of granular sorbents in water treatment is in packed-bed configuration, where contaminated water is purified by passing it through a sorbent-containing column. Therefore, the translational relevance of granular sorbents is heavily determined by their performance in packed-bed configuration. Rapid Small-Scale Column Tests (RSSCTs) are a validated method to probe resin performance in a flow-through, packed-bed column geometry (Crittenden et al., 1991), where the figure of merit is the number of bed volumes of water that pass through the resin before 10% of the influent solute is detected in the effluent water (Park et al., 2020). We used RSSCTs to evaluate the performance of an IF formulation with high performance in batch configuration (i.e., IF-8) and Purolite 694AE IX resin (Figure 16). The influent water was composed of conventional settled water spiked with environmentally relevant levels of PFOA, PFHxA, and GenX ($[PFAS]_0$ = 500 ng/L each).

Neither column exceeded 10% breakthrough of the long-chain PFOA over 150,000 bed volumes. The enhanced performance of the IF was demonstrated by their selectivity for short-chain PFAS, PFHxA and GenX. These two PFAS demonstrated breakthrough for the IX resin at approximately 50,000 bed volumes of water. In contrast, the RSSCT that contained IF-8 displayed no breakthrough of either PFHxA or GenX up to 180,000 bed volumes, which corresponds to 375 days of simulated continuous operation in a pilot-scale treatment plant.

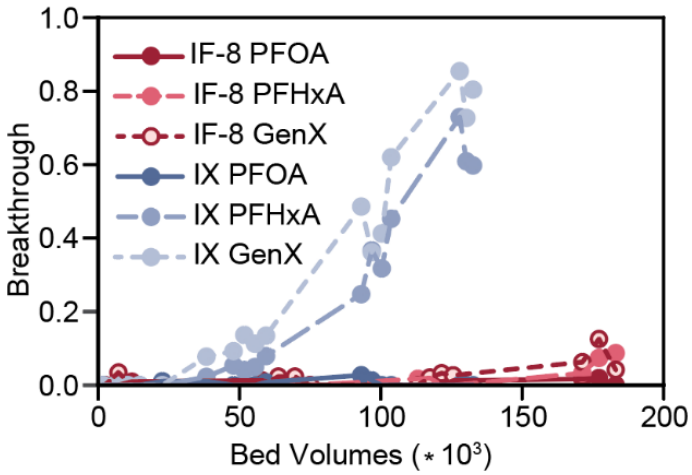

Figure 16. Rapid small scale column tests (RSSCTs) results of IF-8 (red traces) and IX (blue traces). IX = Purolite PFA694AE. Settled conventional water, OWASA, Chapel Hill, NC. $[PFAS]_0$ = 500 ng/L each. Breakthrough = $[PFAS]_{effluent}$ / $[PFAS]_0$.

3.7.4 Packed-bed tests – 2nd generation ionic fluorogels

Results of an RSSCT conducted with IF 2-3, Calgon F400, and PSR2+ are shown in Figure 17. For PFAS of the same length, sulfonates took longer to breakthrough than carboxylic acids (e.g., PFOS longer than PFOA, PFHxS longer than PFHxA). Similarly, longer chain compounds (i.e., PFOA, PFOS) took longer to break through than shorter chain compounds (i.e., PFHxA, PFHxS). PSR2+ was the best performing material, followed by IF 2-3 and GAC. Notably, for FVE-IFs, the breakthrough time for sulfonates increased with decreasing chain length in the order PFOS, PFHxS, and PFBS.

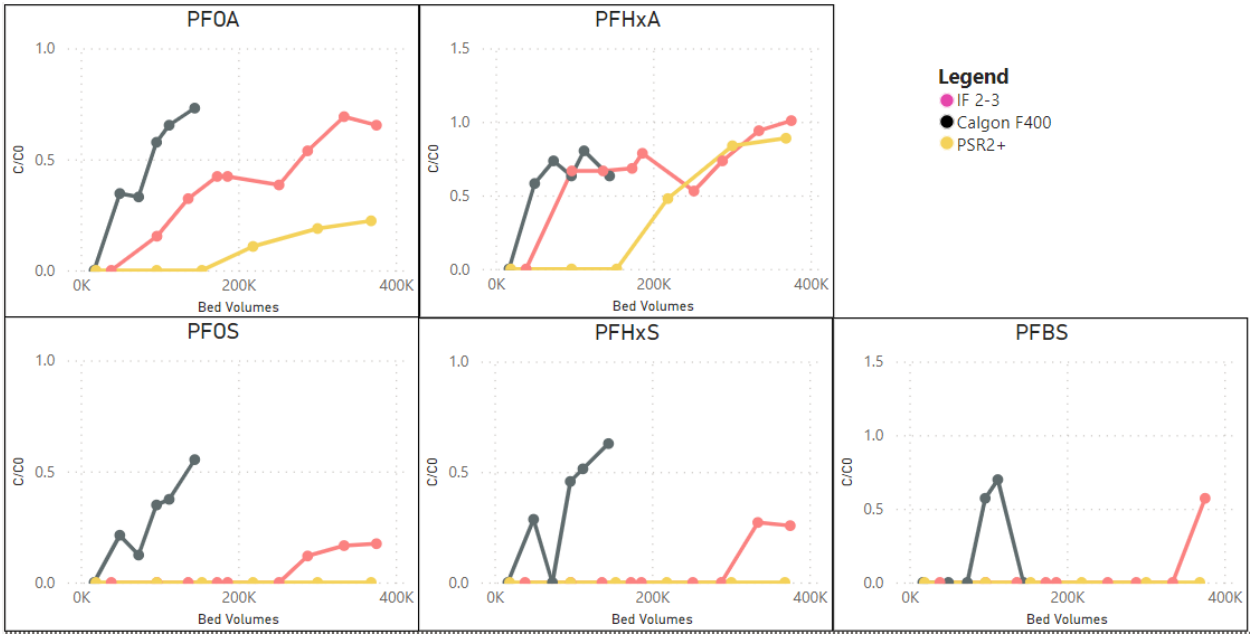

Figure 17. Rapid small scale column tests (RSSCTs) results of IF 2-3 (pink traces), Calgon F400 (black traces), and PSR2+ (yellow traces). Settled conventional water, OWASA, Chapel Hill, NC. Background PFAS concentrations (no spiked PFAS).

4. Conclusions

Hydrolytically stable IFs warrant further development as high-performing materials for the remediation of both legacy and emerging anionic PFAS from water. The design and synthesis of a library of materials indicated that changes in network architecture translate to large differences in PFAS remediation in simulated natural water, while careful end group modification improves hydrolytic stability. These IFs remove a structurally diverse mixture of anionic PFAS at environmentally relevant concentrations from natural waters under batch equilibrium adsorption conditions, which enabled the identification of relationships between PFAS chemical structure and adsorption efficiency. One IF (IF-8) demonstrated superior performance in a flow-through column geometry for the removal of short-chain PFAS from natural water compared with a commercial ion exchange resin, thus indicating the potential of this material to provide a solution for PFAS remediation that is superior and/or complementary to state-of-the-art technologies. Use of FVEs instead of PFPEs in the fluorous backbone structure of the resins to take advantage of more stable and cost accessible building blocks yielded resins with shorter breakthrough times in packed-bed tests which were intermediate between those of a leading commercial resin (PSR2+) and a leading granular activated carbon (F400). Our results indicate

that optimizing the synthesis and processing procedure for the 2nd generation IFs (i.e., FVE-IFs) may further improve PFAS removal performance.

5. Recommendations

The influence of sorbent architecture on PFAS sorption warrants further investigation. Specifically, alterations in crosslink density and thermomechanical properties of the matrix such as glass transition temperature (i.e., backbone rigidity) and swelling likely impact PFAS sorption ability. Furthermore, the chemical identity of the fluorinated polymer backbone led to varied PFAS sorption. A systematic study of the interactions between PFPE and PFAS, FVE and PFAS, PFPE and organic matter or competing ions, and FVE and organic matter or competing ions, is warranted. Understanding the beneficial properties of each polymer class will enable rational design of fluorinated sorbents for PFAS removal which leverage cost-effective starting materials and are highly scalable and efficient.

Results presented here showed that sorbent capacity was highly dependent on the water matrix in which it was tested. The concentrations of sorbates which compete with PFAS, such as TOC and nitrate, were negatively correlated with PFAS removal. Characterizing which fraction of natural organic matter fouls different sorbents could lead to organics removal processes that are optimized for extending sorbent life. Likewise, for wastewater treatment plants with high effluent nitrate, better understanding the competition from nitrate would inform whether denitrification may serve dual benefits of nutrient reduction and extending sorbent life. Advancing the knowledge of how competing sorbate concentrations affect PFAS removal capacity could assist in the design of novel sorbents and assist water utilities and design engineers in optimizing pretreatment processes.

References

Alaaeddine, A., Boschet, F., Ameduri, B., and Boutevin, B. (2012). Synthesis and characterization of original alternated fluorinated copolymers bearing glycidyl carbonate side groups. Journal of Polymer Science Part A: Polymer Chemistry 50, 3303–3312. doi: https://doi.org/10.1002/pola.26112.

Alaaeddine, A., Couture, G., and Ameduri, B. (2013a). An efficient method to synthesize vinyl ethers (VEs) that bear various halogenated or functional groups and their radical copolymerization with chlorotrifluoroethylene (CTFE) to yield functional poly(VE-alt-CTFE) alternated copolymers. Polymer Chemistry 4, 4335–4347. doi: 10.1039/C3PY00443K.

Alaaeddine, A., Hess, A., Boschet, F., Allcock, H., and Ameduri, B. (2013b). Synthesis and characterization of novel alternating fluorinated copolymers bearing oligo(ethylene oxide) side chains. Journal of Polymer Science Part A: Polymer Chemistry 51, 977–986. doi: https://doi.org/10.1002/pola.26463.

ASTM International (2021). ASTM D6586-03 - Standard Practice for the Prediction of Contaminant Adsorption on GAC in Aqueous Systems Using Rapid Small-Scale Column Tests. Available at: https://www.astm.org/d6586-03r21.html.

Barnes, G. (2020a). How Long Will It Take to Rid PFAS from Private Wells? Available at: https://www.northcarolinahealthnews.org/2020/04/07/pfas-private-wells/.

Barnes, G. (2020b). New DEQ Data Show ‘Staggering’’ Levels of PFAS in Cape Fear River Basin.’ Available at: https://www.northcarolinahealthnews.org/2020/02/03/new-deq-data-show-high-levels-of-pfas-in-cape-fear-river-basin/.

Barry, V., Winquist, A., and Steenland, K. (2013). Perfluorooctanoic acid (PFOA) exposures and incident cancers among adults living near a chemical plant. Environ. Health Perspect. 121, 1313–1318. doi: doi:10.1289/ehp.1306615.

Boone, J. S., Vigo, C., Boone, T., Byrne, C., Ferrario, J., Benson, R., et al. (2019). Per- and polyfluoroalkyl substances in source and treated drinking waters of the United States. Sci. Total Environ. 653, 359–369. doi: https://doi.org/10.1016/j.scitotenv.2018.10.245.

Boschet, F., and Ameduri, B. (2014). Copolymers of chlorotrifluoroethylene: Synthesis, properties, and applications. Chemical Reviews 114, 927–980. doi: 10.1021/cr2002933.

Capello, C., Fischer, U., and Hungerbühler, K. (2007). What is a Green Solvent? A Comprehensive Framework for the Environmental Assessment of Solvents. Green Chem. 9, 927–934. doi: 10.1039/B617536H.

City of Raleigh (2020). City of Raleigh: Perfluorinated Compounds Data Results. Available at: https://cityofraleigh0drupal.blob.core.usgovcloudapi.net/drupal-prod/COR25/Perfluorinated.

Couture, G., Alaaeddine, A., Boschet, F., and Ameduri, B. (2011). Polymeric materials as anion-exchange membranes for alkaline fuel cells. Progress in Polymer Science 36, 1521–1557. doi: https://doi.org/10.1016/j.progpolymsci.2011.04.004.

Couture, G., Campagne, B., Alaaeddine, A., and Améduri, B. (2013). Synthesis and characterizations of alternating co- and terpolymers based on vinyl ethers and chlorotrifluoroethylene. Polymer Chemistry 4, 1960–1968. doi: 10.1039/C2PY20977B.

Couture, G., Ladmiral, V., and Améduri, B. (2015). Methods to prepare quaternary ammonium groups-containing alternating poly(chlorotrifluoroethylene-alt-vinyl ether) copolymers. RSC Advances 5, 10243–10253. doi: 10.1039/C4RA09238D.

Crittenden, J. C., Reddy, P. S., Arora, H., Trynoski, J., Hand, D. W., Perram, D. L., et al. (1991). Predicting GAC Performance with Rapid Small-scale Column Tests. J. AWWA 83, 77–87. doi: https://doi.org/10.1002/j.1551-8833.1991.tb07088.x.

Cui, J., Gao, P., and Deng, Y. (2020). Destruction of Per- and Polyfluoroalkyl Substances (PFAS) with Advanced Reduction Processes (ARPs): A Critical Review. Environ. Sci. Technol. 54, 3752–3766. doi: 10.1021/acs.est.9b05565.

Dams, R., and Hintzer, K. (2016). Fluorinated Polymers: Volume 2: Applications.

Dudley, L. A., Arevalo, E. C., and Knappe, D. L. U. (2015). Removal of perfluoroalkyl substances by PAC adsorption and anion exchange. Denver, Colorado: The Water Research Foundation Available at: https://www.waterrf.org/research/projects/removal-perfluoroalkyl-substances-pac-adsorption-and-anion-exchange.

Dukes, T. (2017). Elevated Levels of Unregulated Chemicals Found in Jordan Lake, Cary Drinking Water. Available at: https://www.wral.com/elevated-levels-of-perfluorinated-chemicals-found-in-cary-drinking-water/17205916/.

Evans, S., Andrews, D., Stoiber, T., and Naidenko, O. (2020). PFAS Contamination of Drinking Water Far More Prevalent Than Previously Reported. Available at: https://www.ewg.org/research/national-pfas-testing/.

Evich, M. G., Davis, M. J. B., McCord, J. P., Acrey, B., Awkerman, J. A., Knappe, D. R. U., et al. (2022). Per- and polyfluoroalkyl substances in the environment. Science (1979) 375, eabg9065. doi: doi:10.1126/science.abg9065.

Grandjean, P., Andersen, E. W., Budtz-Jørgensen, E., Nielsen, F., Mølbak, K., Weihe, P., et al. (2012). Serum vaccine antibody concentrations in children exposed to perfluorinated compounds. JAMA 307, 391–397. doi: 10.1001/jama.2011.2034.

Hamiye, R., Alaaeddine, A., Awada, M., Campagne, B., Caillol, S., Guillaume, S. M., et al. (2014). From glycidyl carbonate to hydroxyurethane side-groups in alternating fluorinated copolymers. Polymer Chemistry 5, 5089–5099. doi: 10.1039/C4PY00547C.

Hopkins, Z. R., Sun, M., DeWitt, J. C., and Knappe, D. R. U. (2018). Recently detected drinking water contaminants: GenX and other per- and polyfluoroalkyl ether acids. J. AWWA 110, 13–28. doi: 10.1002/awwa.1073.

Kumarasamy, E., Manning, I. M., Collins, L. B., Coronell, O., and Leibfarth, F. A. (2020). Ionic Fluorogels for Remediation of Per-and Polyfluorinated Alkyl Substances from Water. ACS Central Sci. 6, 487–492. doi: 10.1021/acscentsci.9b01224.

Lee, J., Lopez, G., Améduri, B., and Seo, M. (2020). Synthesis of Heterograft Copolymers with a Semifluorinated Backbone by Combination of Grafting-through and Grafting-from Polymerizations. Macromolecules. doi: 10.1021/acs.macromol.9b02493.

Li, D., and Liao, M. (2017). Dehydrofluorination mechanism, structure and thermal stability of pure fluoroelastomer (poly(VDF-ter-HFP-ter-TFE) terpolymer) in alkaline environment. Journal of Fluorine Chemistry 201, 55–67. doi: https://doi.org/10.1016/j.jfluchem.2017.08.002.

Li, D., and Liao, M. (2018). Study on the dehydrofluorination of vinylidene fluoride (VDF) and hexafluoropropylene (HFP) copolymer. Polymer Degradation and Stability 152, 116–125. doi: https://doi.org/10.1016/j.polymdegradstab.2018.04.008.

Liu, L., Lu, D., Wang, H., Dong, Q., Wang, P., and Bai, R. (2011). Living/controlled free radical copolymerization of chlorotrifluoroethene and butyl vinyl ether under 60Co γ-ray irradiation in the presence of S-benzyl O-ethyl dithiocarbonate. Chemical Communications 47, 7839–7841. doi: 10.1039/C1CC11749A.

MacDonald Gibson, J., and Pieper, K. J. (2017). Strategies to improve private-well water quality: A North Carolina perspective. Environ. Health Perspect. 125, 76001. doi: 10.1289/EHP890.

McCord, J. P., Strynar, M. J., Washington, J. W., Bergman, E. L., and Goodrow, S. M. (2020). Emerging Chlorinated Polyfluorinated Polyether Compounds Impacting the Waters of Southwestern New Jersey Identified by Use of Nontargeted Analysis. Environ. Sci. Technol. Lett. 7, 903–908. doi: 10.1021/acs.estlett.0c00640.

Mohammad, S. A., Shingdilwar, S., Banerjee, S., and Ameduri, B. (2020). Macromolecular engineering approach for the preparation of new architectures from fluorinated olefins and their applications. Progress in Polymer Science 106, 101255. doi: 10.1016/j.progpolymsci.2020.101255.

Najm, I., Gallagher, B., Vishwanath, N., Blute, N., Gorzalski, A., Feffer, A., et al. (2021). Per- and Polyfluoroalkyl Substances Removal with Granular Activated Carbon and a Specialty Adsorbent: A Case Study. AWWA Water Sci. 3. doi: 10.1002/aws2.1245.

National Institute of Environmental Health Sciences (2022). Per- and Polyfluoroalkyl Substances. Available at: https://www.niehs.nih.gov/health/topics/agents/pfc/index.cfm.

North Carolina Division of Water Resources (2018). DEQ GenX Update House Select Committee on River Water Quality. Available at: https://webservices.ncleg.gov/ViewDocSiteFile/45963.

North Carolina PFAS Testing Network (2022). What are the Health Effects of PFAS? Available at: https://ncpfastnetwork.com/printed-materials/.

Park, M., Wu, S., Lopez, I. J., Chang, J. Y., Karanfil, T., and Snyder, S. A. (2020). Adsorption of Perfluoroalkyl Substances (PFAS) in Groundwater by Granular Activated Carbons: Roles of Hydrophobicity of PFAS and Carbon Characteristics. Water Res. 170. doi: 10.1016/j.watres.2019.115364.

Rahman, M. F., Peldszus, S., and Anderson, W. B. (2014). Behaviour and fate of perfluoroalkyl and polyfluoroalkyl substances (PFASs) in drinking water treatment: A review. Water Res. 50, 318–340. doi: https://doi.org/10.1016/j.watres.2013.10.045.

Ross, K. (2020). Forever Chemicals: PFAS Regulation Lags in NC as More Evidence Emerges. Available at: https://carolinapublicpress.org/29932/forever-chemicals-pfas-regulation-lags-in-nc-as-more-evidence-emerges/.

Santhosh Kumar, K. S., and Ameduri, B. (2010). Synthesis and characterization of epoxy functionalized cooligomers based on chlorotrifluoroethylene and allyl glycidyl ether. Journal of Polymer Science Part A: Polymer Chemistry 48, 3587–3595. doi: https://doi.org/10.1002/pola.24138.

Schaefer, C. E., Nguyen, D., Ho, P., Im, J., and Leblanc, A. (2019). Assessing Rapid Small-Scale Column Tests for Treatment of Perfluoroalkyl Acids by Anion Exchange Resin. Ind. Eng. Chem. Res. 58, 9701–9706. doi: 10.1021/acs.iecr.9b00858.

Scruggs, S. (2019). PFAS - A Problem in North Carolina Drinking Water. Available at: https://factor.niehs.nih.gov/2019/3/feature/2-feature-pfas/index.htm.

Seymour Johnson Air Force Base (2019). 2018 Annual Drinking Water Quality Report, Seymour Johnson Air Force Base. Available at: https://www.seymourjohnson.af.mil/Portals/105/2018.

Southern Environmental Law Center (2019). Filing Moves to Stop PFAS Pollution from Central N.C. Wastewater Treatment Plants. Available at: https://www.southernenvironment.org/news-and-press/news-feed/filing-moves-to-stop-pfas-pollution-from-central-n.c-wastewater-treatment-plants.

Sun, M., Arevalo, E., Strynar, M., Lindstrom, A., Richardson, M., Kearns, B., et al. (2016). Legacy and emerging perfluoroalkyl substances are important drinking water contaminants in the Cape Fear River Watershed of North Carolina. Environ. Sci. Technol. Lett. 3, 415–419. doi: 10.1021/acs.estlett.6b00398.

Swenson, H., and Stadie, N. P. (2019). Langmuir's Theory of Adsorption: A Centennial Review. Langmuir 35, 5409–5426. doi: 10.1021/acs.langmuir.9b00154.

United States Environmental Protection Agency (2022a). Basic Information on PFAS. Available at: https://www.epa.gov/pfas/basic-information-pfas.

United States Environmental Protection Agency (2022b). Lifetime Drinking Water Health Advisories for Four Perfluoroalkyl Substances (FRL 9855–01–OW. FR Doc. 2022–13158 Filed 6–17–22). Available at: https://www.govinfo.gov/content/pkg/FR-2022-06-21/pdf/2022-13158.pdf.

United States Environmental Protection Agency (2022c). USEPA Occurrence Data for the Unregulated Contaminant Monitoring Rule. doi: https://www.epa.gov/dwucmr/occurrence-data-unregulated-contaminant-monitoring-rule.

United States Environmental Protection Agency (2023). PFAS National Primary Drinking Water Regulation Rulemaking (40 CFR Parts 141 and 142) [EPA–HQ–OW–2022–0114; FRL 8543–01–OW]. Fed Regist 88, 18638–18754. Available at: https://www.govinfo.gov/content/pkg/FR-2023-03-29/pdf/2023-05471.pdf [Accessed November 28, 2023].

Valade, D., Boschet, F., and Améduri, B. (2009). Synthesis and modification of alternating copolymers based on vinyl ethers, chlorotrifluoroethylene, and hexafluoropropylene. Macromolecules 42, 7689–7700. doi: 10.1021/ma900860u.

Valade, D., Boschet, F., and Ameduri, B. (2010). Grafting polymerization of styrene onto alternating terpolymers based on chlorotrifluoroethylene, hexafluoropropylene, and vinyl ethers, and their modification into ionomers bearing ammonium side-groups. Journal of Polymer Science Part A: Polymer Chemistry 48, 5801–5811. doi: https://doi.org/10.1002/pola.24388.

Wang, P., Dai, J., Liu, L., Dong, Q., Jin, B., and Bai, R. (2013). Xanthate-mediated living/controlled radical copolymerization of hexafluoropropylene and butyl vinyl ether under 60Co γ-ray irradiation and preparation of fluorinated polymers end-capped with a fluoroalkyl sulfonic acid group. Polymer Chemistry 4, 1760–1764. doi: 10.1039/C3PY21158D.

Washington, J. W., Rosal, C. G., McCord, J. P., Strynar, M. J., Lindstrom, A. B., Bergman, E. L., et al. (2020). Nontargeted Mass-spectral Detection of Chloroperfluoropolyether Carboxylates in New Jersey Soils. Science (1979) 368, 1103–1107. doi: 10.1126/science.aba7127.

World Population Review (2022). Median Household Income by State 2021. Available at: https://worldpopulationreview.com/state-rankings/median-household-income-by-state.

Yu, J., Lv, L., Lan, P., Zhang, S., Pan, B., and Zhang, W. (2012). Effect of Effluent Organic Matter on the Adsorption of Perfluorinated Compounds onto Activated Carbon. J. Hazard. Mater. 225–226, 99–106. doi: https://doi.org/10.1016/j.jhazmat.2012.04.073.

Zeng, C., Atkinson, A., Sharma, N., Ashani, H., Hjelmstad, A., Venkatesh, K., et al. (2020). Removing Per- and Polyfluoroalkyl Substances from Groundwaters Using Activated Carbon and Ion Exchange Resin Packed Columns. AWWA Water Sci. 2. doi: 10.1002/aws2.1172.

Appendix 1. Alphabetical List of Abbreviations and Symbols, with Definitions

Symbols	
C_0	Initial concentration of PFAS
C_t	Residual concentration of PFAS
G’	Elastic modulus
G’’	Loss modulus
K_F	Freundlich constant
K_L	Equilibrium constant
m/z	Mass-to-charge ratio
n	Intensity of sorption
Q_m	Maximum sorption capacity at equilibrium
T_g	Glass transition temperature
Abbreviations	
AIBN	Azobisisobutyronitrile
BV	Bed volume
CD	Constant diffusivity
CF_2	Difluoromethylene
CF_2CF_2O	Tetrafluoroethylene glycol
CF_2O	Difluoromethylene glycol
DSC	Differential scanning calorimetry
E10H	Fluorolink®E10H
EBCT	Empty bed contact time
EPA	Environmental Protection Agency
EtOH	Ethanol
FTEG	Fluorinated tetraethylene glycol
FTIR	Fourier-transform infrared
GAC	Granular activated carbon
GenX	Perfluoro-2-methyl-3-oxahexanoic acid
H_2O	Water
HLR	Hydraulic loading rate
HPLC	High performance liquid chromatography
HydroEve	2,2,3,3-Tetrafluoro-3-{[1,1,1,2,3,3-hexafluoro-3-(1,2,2,2-tetrafluoroethoxy)propan-2-yl]oxy}propanoic acid
IX	Ion-exchange resin
IF	Ionic fluorogel
IR	Infrared

LCMS	Liquid chromatography mass spectrometry
M3PFBS	Sodium perfluoro-1-[2,3,4-$^{13}C_3$]butanesulfonate
M3PFHxS	Sodium perfluoro-1-[1,2,3-$^{13}C_3$]hexanesulfonate
M4PFBA	Perfluoro-n-[$^{13}C_4$]butanoic acid
M4PFHpA	Perfluoro-n-[1,2,3,4-$^{13}C_4$]heptanoic acid
M5PFHxA	Perfluoro-n-[1,2,3,4,6-$^{13}C_5$]hexanoic acid
M5PFPeA	Perfluoro-n-[$^{13}C_5$]pentanoic acid
M6PFDA	Perfluoro-n-[1,2,3,4,5,6-$^{13}C_6$]decanoic acid
M8PFOA	Perfluoro-n-[$^{13}C_8$]octanoic acid
M8PFOS	Sodium perfluoro-1-[$^{13}C_8$]octanesulfonate
M9PFNA	Perfluoro-n-[$^{13}C_9$]nonanoic acid
MeOH	Methanol
NaCl	Sodium chloride
Nafion Byproduct 2	1,1,2,2-Tetrafluoro-2-{[1,1,1,2,3,3-hexafluoro-3-(1,2,2,2-tetrafluoroethoxy)propan-2-yl]oxy}ethane-1-sulfonic acid
$NaHCO_3$	Sodium bicarbonate
NaOH	Sodium hydroxide
NC	North Carolina
NVHOS	1,1,2,2-Tetrafluoro-2-(1,2,2,2-tetrafluoroethoxy)ethane-1-sulfonic acid
OWASA	Orange Water and Sewer Authority
PEPA	2,3,3,3-Tetrafluoro-2-(pentafluoroethoxy)propanoic acid
PFAS	Per- and polyfluoroalkyl substances
PFBA	Perfluorobutanoic acid
PFBS	Potassium perfluorobutanesulfonate
PFCA	Perfluoroalkylcarboxylic acid
PFDA	Perfluorodecanoic acid
PFEA	Perfluoroalkyl ether acid
PFHpA	Perfluoroheptanoic acid
PFHxA	Perfluorohexanoic acid
PFHxS	Sodium perfluorohexanesulfonate
PFMOAA	Difluoro(perfluoromethoxy)acetic acid
PFNA	Perfluorononanoic acid
PFO2HxA	Perfluoro-3,5-dioxahexanoic acid
PFO3OA	Perfluoro-3,5,7-trioxaoctanoic acid

PFO4DA	Perfluoro-3,5,7,9-butaoxadecanoic acid
PFO5DA	Perfluoro-3,5,7,9,11-pentaoxadodecanoic acid
PFOA	Perfluorooctanoic acid
PFOS	Perfluorooctanesulfonic acid
PFPE	Perfluoropolyether
PFPeA	Perfluoropentanoic acid
PFS	Pentafluorostyrene
PFSA	Perfluoroalkylsulfonate
PMPA	Perfluoro-2-(perfluoromethoxy)propanoic acid
PP	Polypropylene
PTFE	Polytetrafluoroethylene
RSSCT	Rapid small-scale column test
SEM	Scanning electron microscopy
TGA	Thermal gravimetric analysis
TOC	Total organic carbon

Appendix 2. Dissemination of Results

Presentations and publications, including theses or dissertations

Manning, I. M.; Chew, N.G.P.; Macdonald, H.P.; Coronell, O.; and Leibfarth, F.A. High-Performance Ionic Fluorogels for PFAS remediation from water (poster). *Presented at the Fluoropolymer 2023 conference*, Denver, CO, June 18-21, 2023.

Leibfarth, F.A. Ionic Fluorogels: A Platform Technology for PFAS Remediation from Water. *Presented at the Fluoropolymer 2023 conference*, Denver, CO, June 18-21, 2023.

Manning, I. M.; Chew, N.G.P.; Macdonald, H.P.; Coronell, O.; and Leibfarth, F.A. Efficient, High-Performance Ionic Fluorogels for PFAS Remediation from North Carolina Waters (oral). *Presented at the American Water Works Association (AWWA) Annual Conference & Expo 2023 (ACE23)*, Toronto, ON, Canada, June 10-13, 2023.

Manning, I.M. Efficient, High-performance Ionic Fluorogels for Remediation of North Carolina Waters. *Presented at the Waters Corporation Seminar: Overcome the Challenges of Environmental Applications Using Advanced Mass Spectrometry*, Morrisville, NC, May 15, 2023.

Manning, I.M.; Chew, N.G.P.; Macdonald, H.P.; Coronell, O.; Leibfarth, F.A. Hydrolytically stable ionic fluorogels for high-performance remediation of per-and polyfluoroalkyl substances (PFAS) from natural water (oral). *Presented at the 25th Annual Water Resources Research Institute (WRRI) Conference*, Raleigh, NC, March 22-23, 2023.

Chung, C. Panelist in PFAS Solutions: A Virtual Panel Session for STEM Educators. *Organized by the UNC-Chapel Hill's Center for Environmental Health and Susceptibility and the Iterative Design to Engage All (IDEA) Learners*. Online, March 1, 2023.

Coronell, O. PFAS removal from water: challenge description, technology fundamentals, and research and translational capacity at UNC. *Presented at the PFAS Characterization, Removal and Replacement Workshop*, Chapel Hill, NC, January 6, 2023.

Leibfarth, F.A. Ionic Fluorogels for PFAS Remediation from Natural Waters. *Presented at the PFAS Characterization, Removal and Replacement Workshop*, Chapel Hill, NC, January 6, 2023.

Coronell, O.; Chung, C. Removing PFAS from North Carolina Waters. *Keynote presentation in University Day at the University of North Carolina*, Chapel Hill, NC, October 12, 2022.

Coronell, O. An innovation for removing 'forever chemicals' from North Carolina waters. *Presented at the Gillings SPH Advisory Council Fall Meeting*, Cary, NC, October 21, 2022.

Manning, I.M. (2022) Ionic fluorogels for remediation of per- and polyfluorinated alkyl substances from water. PhD Dissertation. University of North Carolina at Chapel Hill, Chapel Hill, NC, US.

Manning, I.M.; Chew, N.G.P.; Macdonald, H.P.; Miller, K.E.; Strynar, M.J.; Coronell, O.; Leibfarth, F.A. (2022) Hydrolytically stable ionic fluorogels for high-performance PFAS remediation from natural water. *Angewandte Chemie International Edition*, *61*, e202208150. DOI: 10.1002/ange.202208150

Manning, I.M.; Kumarasamy, E.; Chew, N.G.P.; Macdonald, H.P.; Collins, L.B.; Coronell, O.; Leibfarth, F.A. Ionic fluorogels for remediation of PFAS from water (oral). *Presented at the 264th Meeting of the American Chemical Society (ACS)*, Chicago, IL, August 21-25, 2022.

Manning, I.M.; Chew, N.G.P.; Macdonald, H.P.; Collins, L.B.; Coronell, O.; Leibfarth, F.A. Ionic fluorogels for remediation of PFAS from water (poster). *Presented at the 3rd National PFAS Conference*, Wilmington, NC, June 15-17, 2022.

Manning, I.M.; Kumarasamy, E.; Chew, N.G.P.; Macdonald, H.P.; Collins, L.B.; Coronell, O.; Leibfarth, F.A. Ionic fluorogels for remediation of PFAS from water (poster). *Presented at the Triangle Soft Matter Symposium*, Durham, NC, May 9, 2022.

Chung, C.; Macdonald, H.P.; Chew, N.G.P.; Manning, I.M.; Coronell, O.; Leibfarth, F. Novel Sorbents for PFAS Water Remediation (poster). *Presented at the Spring 2022 UNC Undergraduate Research Symposium*, Chapel Hill, NC, April 25, 2022**.**

Leibfarth, F.A.; Coronell, O. Ionic fluorogels as sorbents for the remediation of PFAS from water (oral). *Presented at the 263rd Meeting of the American Chemical Society (ACS)*, San Diego, CA, March 20-24, 2022.

Patents, data sets, or web sites

N/A.

Efforts at technology transfer or communication of results to end users, policy makers, or others (beyond, or based on, the items from the two bullets above)

The PIs have disseminated to NC policymakers and water treatment utilities across the state the results obtained with the ionic fluorogel technology. Follow up funding from the State via the North Carolina Collaboratory has been secured.

Appendix 3. Peer-reviewed Manuscript and Corresponding Supporting Information

Manning, I.M.; Chew, N.G.P.; Macdonald, H.P.; Miller, K.E.; Strynar, M.J.; Coronell, O.; Leibfarth, F.A, *Angew. Chem. Int. Ed.* 2022**,** *61,* e202208150 (DOI: 10.1002/anie.202208150)